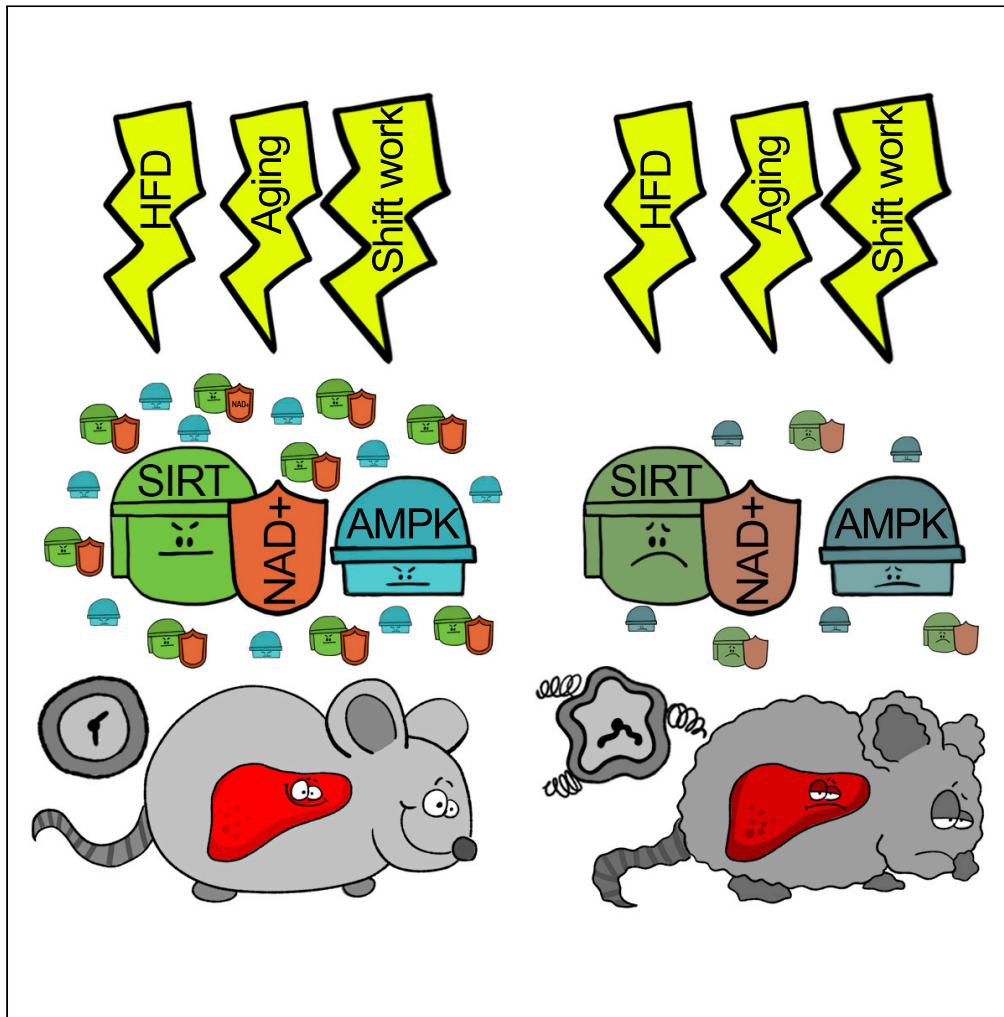**Article**

Aging affects circadian clock and metabolism and modulates timing of medication

Mehrshad Sadria,
Anita T. Layton

msadria@uwaterloo.ca

HIGHLIGHTS

We model the circadian pathway coupled with the mouse liver metabolism pathways

Model reveals the mechanisms by which variations in food intake disrupt the clock

Reduced NAD+ and SIRT1 levels may shorten the circadian period in aged rodents

Dosing schedules are identified to maximize the efficacy of anti-aging medications

Article

Aging affects circadian clock and metabolism and modulates timing of medication

Mehrshad Sadria[1,3,*] and Anita T. Layton[1,2]

SUMMARY

Aging is associated with impairments in the circadian rhythms, and with energy deregulation that affects multiple metabolic pathways. The goal of this study is to unravel the complex interactions among aging, metabolism, and the circadian clock. We seek to identify key factors that inform the liver circadian clock of cellular energy status and to reveal the mechanisms by which variations in food intake may disrupt the clock. To address these questions, we develop a comprehensive mathematical model that represents the circadian pathway in the mouse liver, together with the insulin/IGF-1 pathway, mTORC1, AMPK, NAD+, and the NAD+ -consuming factor SIRT1. The model is age-specific and can simulate the liver of a young mouse or an aged mouse. Simulation results suggest that the reduced NAD+ and SIRT1 bioavailability may explain the shortened circadian period in aged rodents. Importantly, the model identifies the dosing schedules for maximizing the efficacy of anti-aging medications.

INTRODUCTION

From bacteria to humans, organisms possess a network of molecular reactions and pathways, the interactions of which form an internal biological clock, known as a circadian clock, which generates biochemical oscillations with a near 24-hr period (Dibner et al., 2010). The circadian system can be divided into two interacting components: the central clock in the suprachiasmatic nucleus (SCN) of the hypothalamus and the peripheral clocks that reside in various tissues throughout the body. The peripheral clocks play an integral and unique role in each of their respective tissues, driving the circadian expression of specific genes involved in a variety of physiological functions. As a whole, the circadian system drives daily oscillation in most physiological functions, including circulating hormones (Kim et al., 2015), cardiac and circulatory function (Millar-Craig et al., 1978; Muller et al., 1985), and core body temperature (Refinetti and Menaker, 1992). The circadian clock can synchronize the timing of physiological processes with cyclic changes in the external environment (called "zeitgebers"), to the advantage of the organism. Light is a major zeitgeber, especially for the SCN; its importance is evinced by the ubiquitous presence of an anticipatory system linking physiology with the light/dark cycle in all species. Other key zeitgebers include temperature, food intake, and exercise. Feeding is a particularly potent zeitgeber for the peripheral circadian clocks such as the liver clock.

The control of the circadian clock over a variety of cellular and circulating metabolites and fuels is well documented. However, that link is more complex than the rhythm simply controlling metabolism. Indeed, studies have pointed to a cyclic relationship wherein the rhythm impacts metabolic activity and metabolism feeds back to impinge upon the rhythm (Roenneberg and Merrow, 1999). Perhaps the best test case to evaluate the link between metabolism and circadian rhythms is the liver, an organ that is critically involved in the primary food response. Cellular metabolism in the liver is markedly affected by changes in feeding status and therefore fluctuates as a function of the day/night cycle in rodents (Robinson et al., 1981; Kaminsky et al., 1984). To complete the cycle of influence, restricted feeding is also known to significantly alter the circadian phase in the liver (Tulsian et al., 2018).

Impairments in circadian rhythms in sleep and behaviors (Kondratova and Kondratov, 2012) are known to occur in aging, although the underlying mechanisms are not well understood. Aging is a multifactorial process characterized by a gradual decline of physiological functions. A series of mechanisms are involved at the molecular, cellular, and tissue levels, which include deregulated autophagy, mitochondrial dysfunction, telomere shortening, oxidative stress, systemic inflammation, and metabolism dysfunction (Riera et al., 2016). The deregulation of these pathways gives rise to cellular senescence, which contributes to aging

[1]Department of Applied Mathematics, University of Waterloo, Waterloo, ON, Canada

[2]Department of Biology, Cheriton School of Computer Science, and School of Pharmacy, University of Waterloo, Waterloo, ON, Canada

[3]Lead contact

*Correspondence: msadria@uwaterloo.ca

phenotype and, eventually, age-related diseases. Aging is associated with a reduction in the cellular concentration of nicotinamide adenine dinucleotide (NAD+), a critical coenzyme for enzymes that fuel reduction-oxidation, and with a decline in the expression of Sirt1, a member of the sirtuin family for which NAD+ is a co-substrate, at the transcriptional and translational levels. (We follow the convention where only the first letter is capitalized in genes, e.g., Sirt1, but all capital letters for proteins, e.g., SIRT1.) Additionally, aging is associated with energy deregulation which affects many pathways such as pyruvate metabolism, the tricarboxylic acid cycle, and insulin.

The interactions among aging, metabolism, and circadian clock are difficult to unravel. Despite the wealth of aging-related data generated by high-throughput genomic and proteomic technologies, some of the molecular mechanisms that mediate key aging effects have yet to be elucidated. The difficulty lies in the complexity of these processes: not only are a large number of genes involved, many with competing roles, but their interactions are complex and often incompletely characterized. Indeed, due to the multiple feedback loops and regulatory mechanisms, it is challenging to understand the biological consequences of gene-expression changes. A promising methodology for interpreting data and untangling the interactions among signaling pathways is computational biology. One such approach is to describe regulatory interactions using ordinary differential equations, which relate changes in the expressions of model variables to other quantities. Simulations can then be conducted to predict how perturbation in one model parameter or variable (or a set of parameters and variables) can affect other variables and overall system behaviors.

The principal goal of this study is to develop a state-of-the-art computational model that couples the metabolism and circadian pathways, to investigate the roles of these pathways in aging and metabolism in mammals. We aim to apply the model to answer important questions: *What are the key factors that advice the liver circadian clock about the cellular nutritional state, and facilitate its entrainment to a feeding schedule? How might variations in daily food intake or nutritional stress disrupt the clock? How do those processes change as one ages? What time of day should one take an anti-aging medication to maximize its efficacy?* To address these questions, we present a comprehensive model that includes (i) the insulin/IGF-1 pathway, which couples energy and nutrient abundance to the execution of cell growth and division, (ii) the mechanistic target of rapamycin complex 1 (mTORC1) and amino acid sensors, (iii) the salvage pathway, which regulates the metabolism of NAD+ and the NAD+ -consuming factor SIRT1, (iv) the energy sensor adenosine monophosphate-activated protein kinase (AMPK), and (v) the circadian pathway in the mouse liver. We formulate the model for a young mouse and an aged mouse, and we apply the model to investigate the synergy among regulators of nutrients, energy, metabolism, and circadian rhythms. Last but not the least, we conduct simulations to assess the effect of dosing schedule on the pharmacodynamics of anti-aging drugs, of which the key molecular target of these drugs is SIRT1. Because SIRT1 is under major influence by the circadian clock (Wallace et al., 2018), the optimal dosing times for these medications remain an essential but unanswered question. The model can be used to aid in the interpretation of time dynamic genomic and proteomic data, and to provide an integrated understanding of the mechanisms that lead the cell to senescence and how this process contributes to aging and age-related diseases.

RESULTS

Model predicts expression time-profiles of core clock genes in the mouse liver

The intricate coupling of the energy and metabolism pathways and the circadian system is represented in the model; see Figure 1. The phosphorylation of mTORC1 elevates BMAL1, whereas BMAL1 and PER2 inhibit mTORC1. As such, the circadian rhythms drive oscillations in phosphorylated mTORC1 level (Figure 2B). The model predicts a phase difference between mTORC1 and Bmal1 mRNA of ∼9 hr. Similar oscillations are seen in other variables in the insulin pathway model. These results were obtained for the "young" model with a constant baseline insulin level.

To assess the validity of the model, we compare the predicted time-profiles of core clock genes with mRNA levels measured in mouse livers (Hughes et al., 2009). In that study, the mice were entrained to a 12:12 light/dark cycle, then put in constant darkness and fed ad libitum. The predicted core clock mRNA time-profiles for Bmal1 (Figure 2A), Per2 (Figure 2C), Cry1 (Figure 2D), Rev-Erb (Figure 2E), and Ror (Figure 2F) all exhibit reasonable agreement with the mouse liver data (closed circles).

As noted above, the model represents bidirectional coupling between mTORC1 and core clock genes. To assess how the fit between model predictions and data is affected, we conducted simulations (1) without
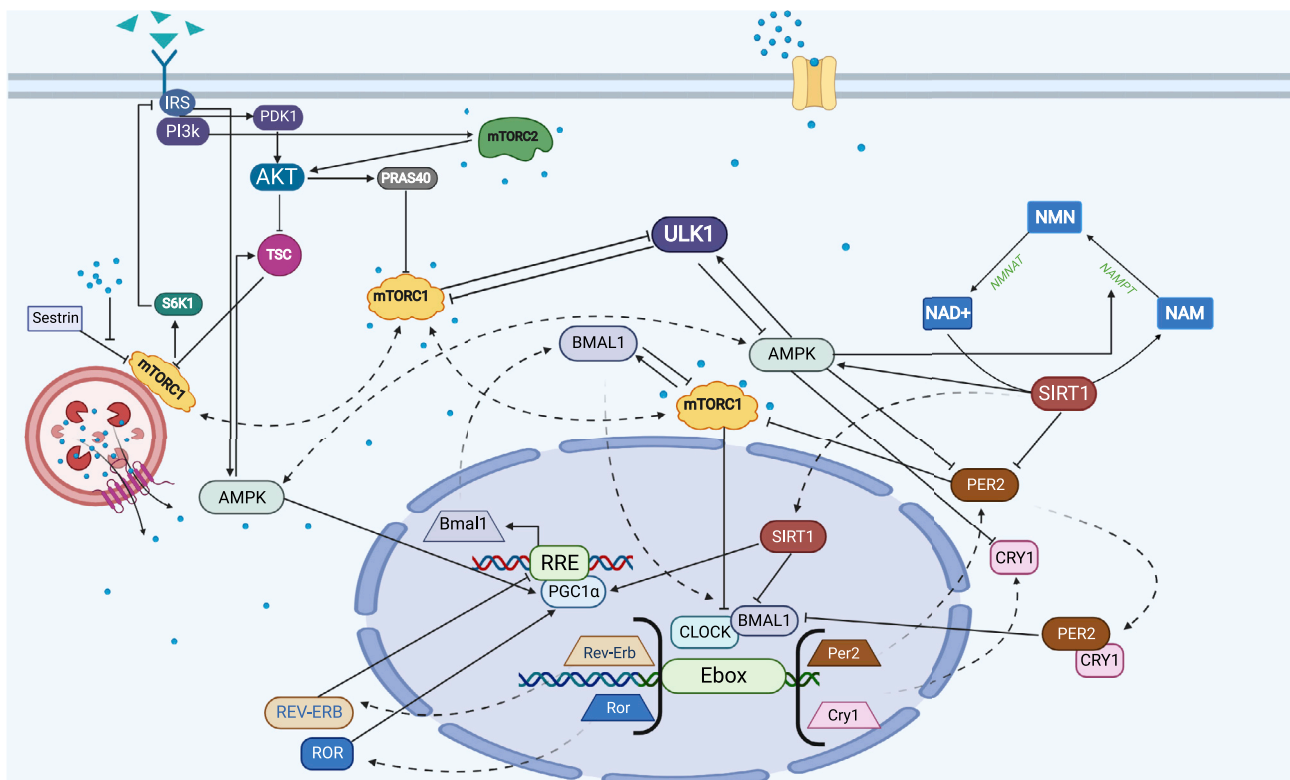
Figure 1. Schematic representation of the circadian clock, energy, and metabolism pathways, and their coupling

Dashed arrows denote protein movements, or the translocation of genes and proteins. Some components in the metabolism pathway may be activated by amino acids, such as leucine (blue circles) and insulin (green triangles). The model represents three distinct areas in the cell: the cytoplasm, lysosome, and the nucleus.

the inhibitory effects of BMAL1 and PER2 on mTORC1, and (2) the without the activating effect of mTORC1 on BMAL1 and CLOCK-BMAL1. In both cases, the predicted core clock gene and mTORC1 profiles deviate markedly from baseline; results are shown in Figure S1 (supplemental information). Without the inhibitory effects of BMAL1 and PER2 on mTORC1, the oscillations in mTORC1 vanish, with mTORC1 attaining elevated steady-state value. The elimination of the activating effect of mTORC1 on BMAL1 and CLOCK-BMAL1 introduces a phase shift in all oscillations (Figure S1).

Effect of feeding on mTORC1 and liver clock genes

The circadian system, metabolism, and feeding are intertwined. To better understand the effect of food on liver circadian rhythms, we simulate a fed-like state and a fasted-like state. Nutrition levels (i.e., insulin and amino acid) are assumed to stay high at the baseline levels in a fed-like state, to stay low in a fasted-like state. When insulin and amino acid levels are low, they are taken to be 10% and 50% of baseline, respectively.

The time-profiles predicted for mTORC1 and key clock proteins are shown in Figure 3 (blue and red curves). mTORC1 is activated by a high-energy diet through the uptake of glucose and amino acids (Figure 3B). At high nutrition levels, the elevated insulin and growth factor levels promote the phosphorylation of Akt, which inhibits TSC1-TSC2 and activates mTORC1. Conversely, in the fast-like state, phosphorylated mTORC1 drops to $1/4$ its value in the fed-like state, and its circadian oscillations essentially vanish. Recall that activation of mTORC1 results in elevated levels of BMAL1. Thus, fasting lowers BMAL1 level (Figure 3C). CLOCK-BMAL and CRY1 are similarly affected, whereas the effect on PER2 is the opposite (Figures 3D–3F).

The above results are obtained for the baseline (young) model. We seek to determine if these effects persist when metabolism changes during aging. To achieve that goal, we formulate an aged model by lowering the mean NAD+ and SIRT1 levels to 30% and 60%, respectively, of the baseline model (Massudi
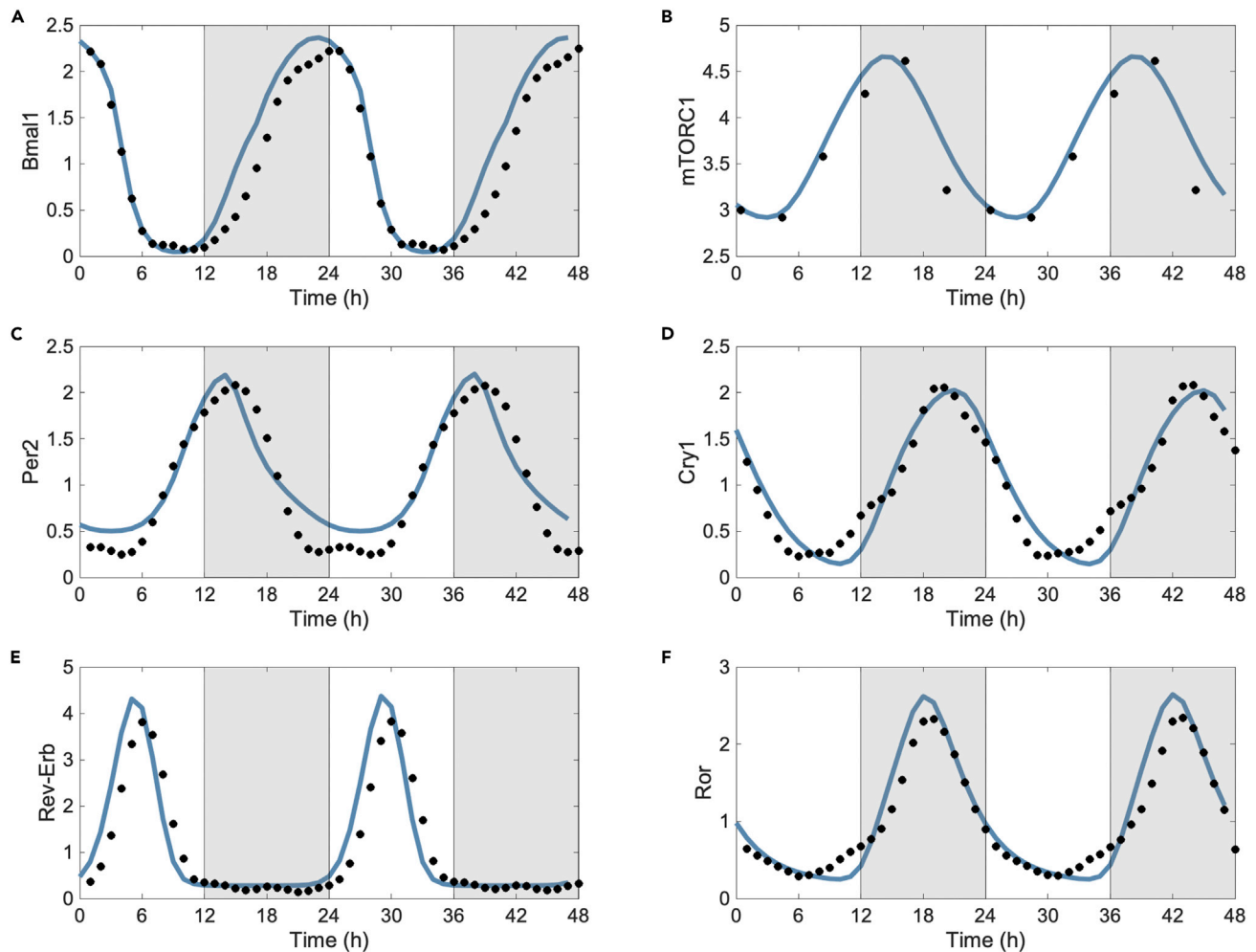
Figure 2. Predicted oscillations in core clock gene and mTORC1 levels
(A) predicted Bmal1 mRNA time profile.
(B) mTORC1 level, driven to oscillate by the clock.
(C–F) predicted Per2, Cry1, Rev-Erb, and Ror time-profiles.
Shown in arbitrary unit. Experimental data are shown in closed circles. Data for Bmal1, Per2, Cry1, Rev-Erb, and Ror are taken from (Woller et al., 2016). Data for pS6K S235, a common readout for mTORC1, is included in panel (B) (Khapre et al., 2014). Comparison between mTORC1 and S6K S235 should be restricted to phase and period, not actual expression value.

et al., 2012a). Qualitatively similar results are obtained for the aged model (shown in Figure S2 in supplemental information).

The liver circadian clock entrains to an altered feeding schedule

Food is known to be a potent zeitgeber for the liver circadian cycle. To assess the effect of an altered feeding schedule on the circadian rhythm, we simulate daytime and nighttime feeding by varying the insulin and amino acid levels during the day. The simulated insulin levels for the different feeding patterns are shown in Figure 3A, green and orange curves. The simulated amino acid levels follow the same trend and vary between 0.5 and 1. The model predicts that variations in nutrition levels yield oscillations in mTORC1 (see explanation above). Nighttime feeding induces a half-day phase shift in the mTORC1 (Figure 3B) relative to the constant fed-like case, and the coupling between mTORC1 and BMAL1 induces a corresponding phase shift in the clock as well (see orange curves in Figures 3C–3F).

These results suggest that the liver circadian clock may entrain to an altered feeding schedule via its coupling with mTORC1. More specifically, results obtained for the four feeding conditions suggest that
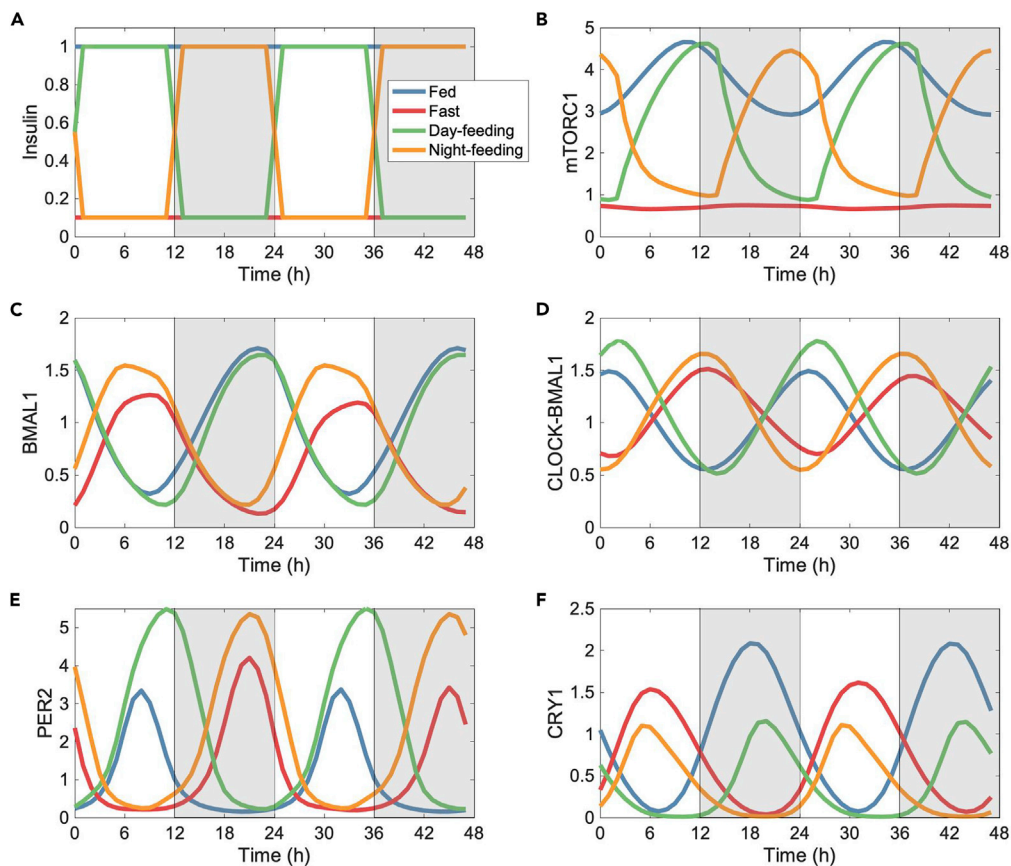
Figure 3. Effects of feeding schedule on mTORC1 and core clock gene levels

(A) insulin levels for a fed-like state (constant at 1), a fasted-like state (constant at 0.1), daytime feeding, and nighttime feeding.

(B) mTORC1 levels, driven to oscillate by the clock and feeding schedule, and elevated at high insulin levels.

(C–F) core clock protein time-profiles.

Shown in arbitrary unit.

without a sufficiently strong activation signal from mTORC1, as in the fast-like state, the model is formulated such that BMAL1 and CRY1 peak around ZT8, whereas PER2 peaks around ZT20. With nighttime feeding, mTORC1 peaks around ZT23, such that its activation of BMAL1 yields a peak around ZT6. Therefore, the fast-like and nighttime feeding cases produce qualitatively similar core clock protein profiles. In contrast, with daytime feeding, mTORC1 level increases during the day, with a peak at ZT12. That shifts the BMAL1 profile by half a day, with a peak now at ZT22. A similar phase relation in the clock gene oscillations is obtained for the fed-like state, indicating that the activating signal from mTORC1 during the day may be a primary determine of the phase dynamics of the clock.

Effect of aging on the circadian clock

As we age, our circadian system undergoes significant changes, such that rhythmic activities such as sleep/wake patterns change markedly, and in many cases become increasingly fragmented. Aging is also associated with the reduction in the cellular concentration of NAD+ and SIRT1 (Satoh et al., 2017). To study the effect of key age-related changes in metabolism on the circadian system, we formulate an aged model by lowering the mean NAD+ and SIRT1 levels to 25% and 40%, respectively, of the baseline (young) model (Massudi et al., 2012a). We acknowledge that aging is associated with a multitude of other physiological changes. But here we focus on the effect of NAD+ and SIRT1, which are known to play an essential role in the mechanism that translates the regulation of energy metabolism into aging and longevity.
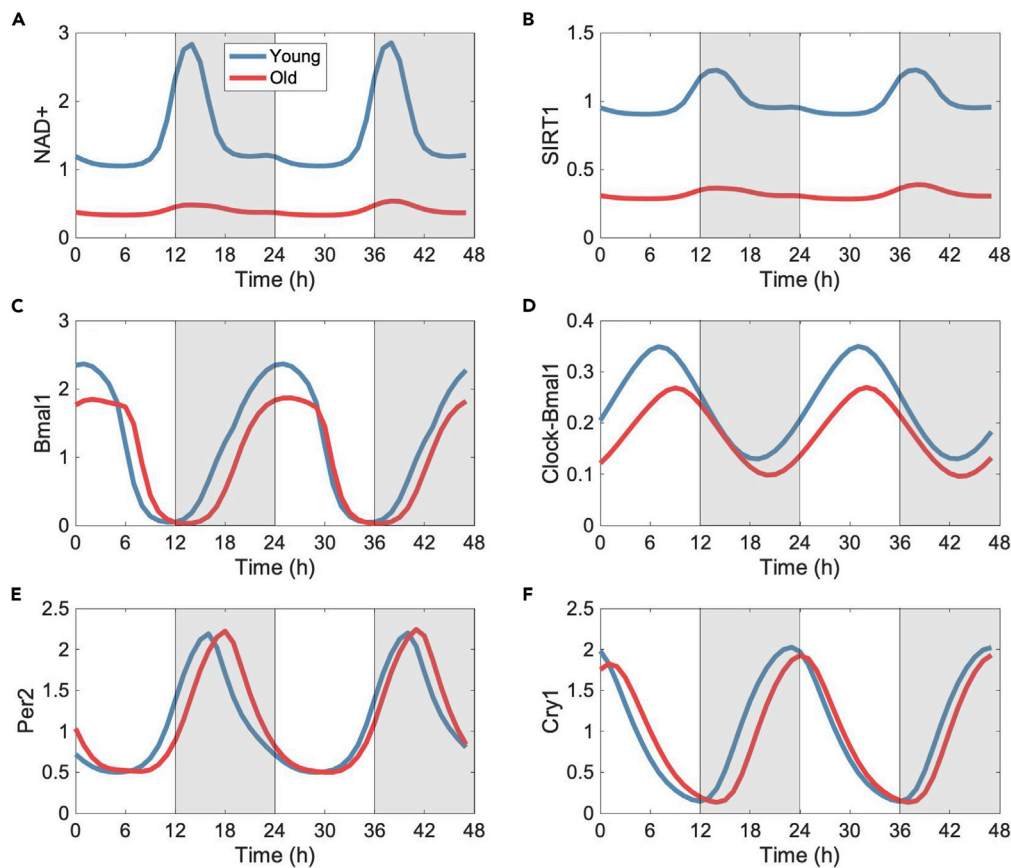
Figure 4. Effect of aging on metabolism and the circadian clock

(A–F) Shown in arbitrary unit. Aging reduces the bioavailability of NAD+ (A) and SIRT1 (B), which lowers Bmal1 (C) and Clock-Bmal1 levels (D) but has a negligible effect on the abundance of Per2 (E) and Cry1 (F). Aging shortens the circadian period.

The resulting time-profiles of core clock genes are shown in Figure 4. SIRT1 deacetylates the liver kinase B1 (LKB1), which stimulates AMPK. Through their actions on PGC1-α, SIRT1 and AMPK raise the level of Bmal1. Thus, the lower SIRT1 and AMPK levels in the aged model yield correspondingly reduce Bmal1 and Clock-Bmal1 (Figures 4C and 4D). Taken in isolation, the lower Clock-Bmal1 level would decrease the generation rates of Per2 and Cry. However, in a competing effect, the lower SIRT1 level in the aged model also inhibits the deacetylation of Clock-Bmal1, thereby accelerating the formation of Per2 and Cry1. These two competing effects result in negligible effects on the abundance of Per2 and Cry1 (Figures 4E and 4F). What is noteworthy is that the lower SIRT1 level shortens the circadian period in the aged model, from the baseline 24 hr–22 hr, consistent with observed age-related disruption in circadian rhythms (Yamazaki et al., 2002; Morin, 1988) (*infra vide*).

Effect of dosing schedule on pharmacodynamics

Resveratrol and other SIRT1-activating compounds (STACs) increase SIRT1 activity and mimic the anti-aging effects of calorie restriction in lower organisms and mice(Howitz et al., 2003). Given the modulation of SIRT1 by the circadian clock and vice versa, we investigate how the dosing schedule may differentially affect the pharmacodynamics of STAC on the young and aged models. The models compute SIRT1 activity as a Michaelis-Menten function of [NAD+]. To simulate the effect of STAC, we reduce the Michaelis-Menten constant K_m (Milne et al., 2007) and vary SIRT1 generation during the day. We compare the cases where the STAC is taken at ZT6, ZT12, and ZT24. The predicted NAD+ time-profiles are shown in Figures 5D and 5G for the young and aged models, respectively. All NAD+ profiles are normalized with respect to the mean NAD+ value in the young model. The corresponding predicted SIRT1 time-profiles are in Figures 5E and 5H, normalized by the mean SIRT1 value in the young model. Recall that NAD+ and SIRT1 levels are
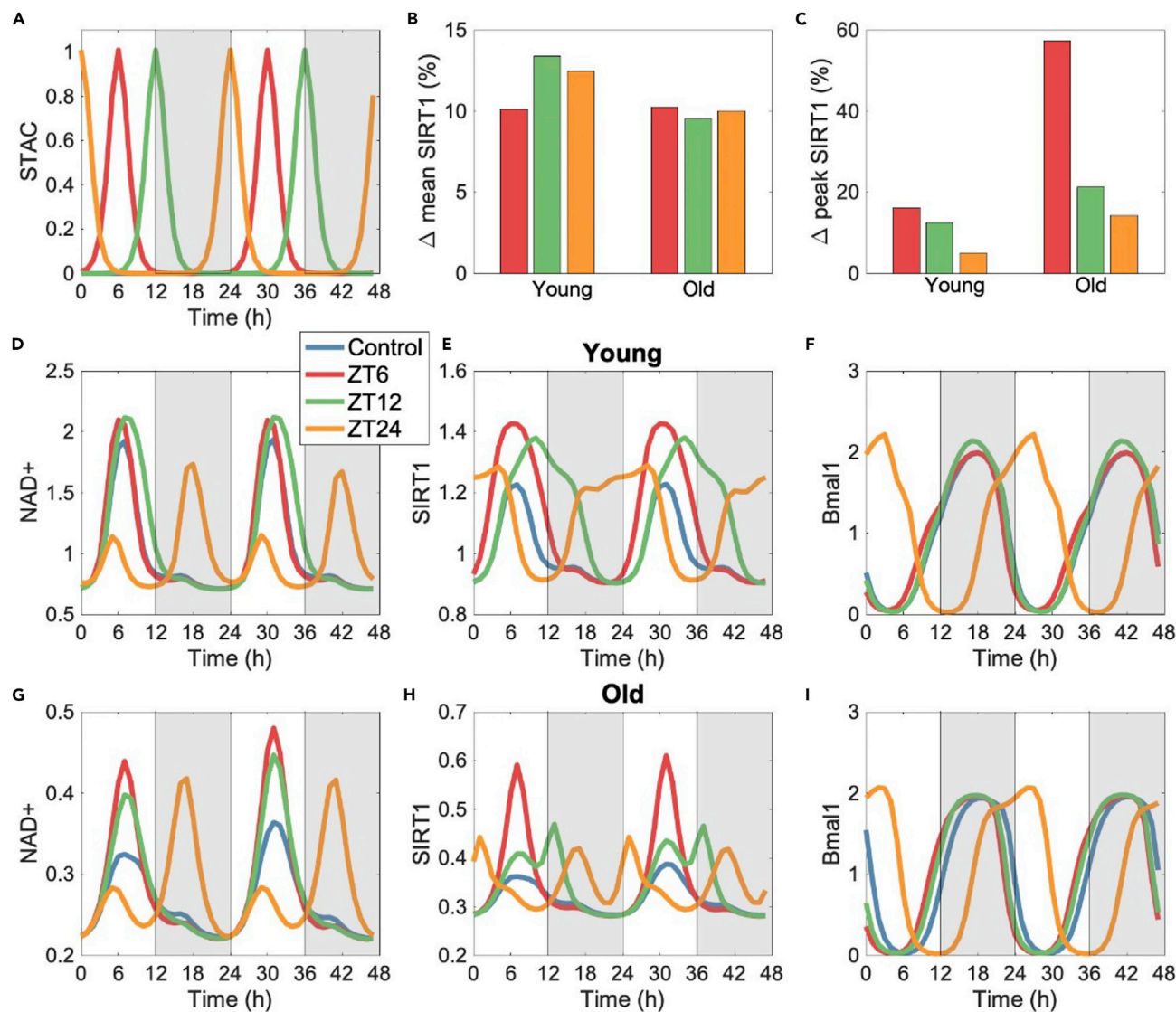
Figure 5. Effect of dosing schedule on STAC efficacy

(A–I) Shown in arbitrary unit. Simulations are conducted for STAC administered at ZT6, ZT12, and ZT24 (A), and in the young model (results in the second row) and aged model (third row). STAC has a major impact on the dynamics of NAD+ (D and G) and SIRT1 (E and H). Dosing schedule has a significant effect on mean SIRT1 in the young model but not the aged model (B), whereas the effect on peak SIRT is significant in the young model and even stronger in the old model (C). Δ mean and peak SIRT1 for the young and aged models are computed as percentage changes with respect to the respective control group (no drug).

attenuated in aging. As a result, the pharmacodynamics of STAC and its dosing schedule differ markedly between the two populations.

The young and aged models exhibit different responses to the dosing schedule. Given that mammalian SIRT1 deacetylates a host of target proteins that are important for apoptosis, the cell cycle, circadian rhythms, mitochondrial function, and metabolism, we will assess drug response using two measures of SIRT1 levels, its mean and peak, computed over a representative circadian period. The peak value is important in threshold-based processes. Relative changes in mean and peak SIRT1 for the young and aged models are given by percentage changes relative to the respective control group (no drug).

In terms of mean SIRT1, the young and aged models exhibit similar relative increases (approximately +10%) when STAC is administered at ZT6, which is the middle of the light cycle and coincides approximately with

the circadian peaks of the NAD+ and SIRT1 in the control group (no drug). (Figure 5). Because baseline SIRT1 is much higher in the young model, the same relative increase implies a much larger net increase in the young model. When administered at ZT12, the beginning of the dark cycle, STAC induces the largest increase in mean SIRT1 in the young model (+13.4%), whereas the analogous response of the aged model is essentially insensitive to the dosing schedule (+9.5%, Figure 5B). When administered at the end of the dark cycle (ZT24), STAC induces +12.7% and +9.8% increases in mean SIRT1 the young and aged models, respectively. In terms of peak SIRT1, drug timing has a significant effect on both the young and aged models (see Figure 5C). The most marked increase in relative peak SIRT1 is obtained when STAC is administered to the aged model at ZT6. Alternative dosing schedules and the young model yield significant but weaker response in peak SIRT1.

Further discussion is warranted for the ZT24 case (dosing at the beginning of the light period). Double peaks emerge in the NAD+ and SIRT1 time-profiles (orange curves in Figures 5D, 5E, 5G, and 5H), with one peak corresponding to the circadian peak, the other to the STAC-induced peak. Also, Bmal1 time-profiles indicate a 7-hr shift in the circadian clock, in both the young and aged models (Figures 5F and 5I). Such a shift may be undesirable.

NAD+ is a central regulator of metabolism, and its decline is linked to DNA damage (Bouchard et al., 2003), metabolic stress, chronic inflammation (Imai and Guarente, 2014), and aging (Braidy et al., 2014; Massudi et al., 2012b). The consumption of nicotinamide riboside (NR), a precursor of NAD+ and is similar to B3, has been proposed as a means to elevate NAD+ levels and to improve healthspan (Yoshino et al., 2018). To represent the effect of NAD+ supplements, we increase the total NAD+ and NAM concentration during specific hours of the day, depending on the dosing schedule (Figures 6A and 6B). We compare the cases where the NAD+ supplements are taken at ZT6, ZT12, and ZT24. The predicted NAD+ and SIRT1 time-profiles are shown in Figure 6 for the young model (panels D and E) and old model (panels G and H).

The model predicts that NAD+ supplements exert the strongest effect, as measured by either mean or peak SIRT1, if taken during the middle of the light cycle, at ZT6, which coincides with the peak of the circadian peak (Figures 6B and 6C). The model predicts that mean SIRT1 increases by 7.5% in the young case and 5.6% in the aged case. If peak SIRT1 is the measure, then a larger increase of 14.2% is predicted in the aged model, compared to 36.0% in the young model. Administering NAD+ supplements at a different hour may generate smaller effect. Taken at ZT12, mean SIRT1 increases by 6.6% in the young model and 3.0% in the aged model (Figure 6B). Unlike the ZT6 case, the ZT12 case results in a smaller increase in peak SIRT1 in the aged model (5.7%), compared to 10.8% in the young model (Figure 6C). Taken at ZT24, mean SIRT1 increases by only 3.9% in the baseline model, but essentially has no response (+0.5%) in the aged model (Figure 6B). Even more remarkably, peak SIRT1 decreases by 7.9% in the aged model (Figure 6C). Furthermore, unlike STAC, taking NAD+ supplements at ZT24 does not result in a phase shift of the circadian rhythms; see Bmal1 time-profiles in Figures 6F and 6I.

DISCUSSION

Metabolism and the circadian rhythms

Early work in mammalian rhythms identified the hypothalamic SCN as the master circadian pacemaker that drives behavioral rhythms (Welsh et al., 2010). Soon after, it was realized that circadian genes expression is by no means limited to the SCN but can be found in cells throughout the body (Dibner et al., 2010). Indeed, the cell-autonomous clock is ubiquitous (Balsalobre et al., 1998; Nagoshi et al., 2004; Yoo et al., 2004), with most peripheral organs and tissues simultaneously exhibiting autonomous circadian oscillations and receiving signals from the SCN. In different cell types, the circadian oscillators respond differently to entraining signals. SCN gene expression responds rapidly to light, a tight coupling that is mediated by the neural connections from the SCN and the retina to the SCN. As a result, SCN gene expression entrains to a shifted light/dark schedule within a day (Yamazaki et al., 2000). Interestingly, while other nonphotic stimuli, like a shifted feeding schedule, can dominate light in entraining behavioral and peripheral rhythms, the SCN is hard-wired to the light/dark rhythm.

Unlike the SCN, light exerts only a weak entraining effect on the liver. Experiments in the rat demonstrate the even after 16 days of an altered light/dark regimen, the liver clock does not completely adapt to the new schedule (Yamazaki et al., 2000). In contrast, feeding is a potent zeitgeber for the liver circadian cycle. A restricted feeding protocol, in which mice are given food access for a limited period during the light
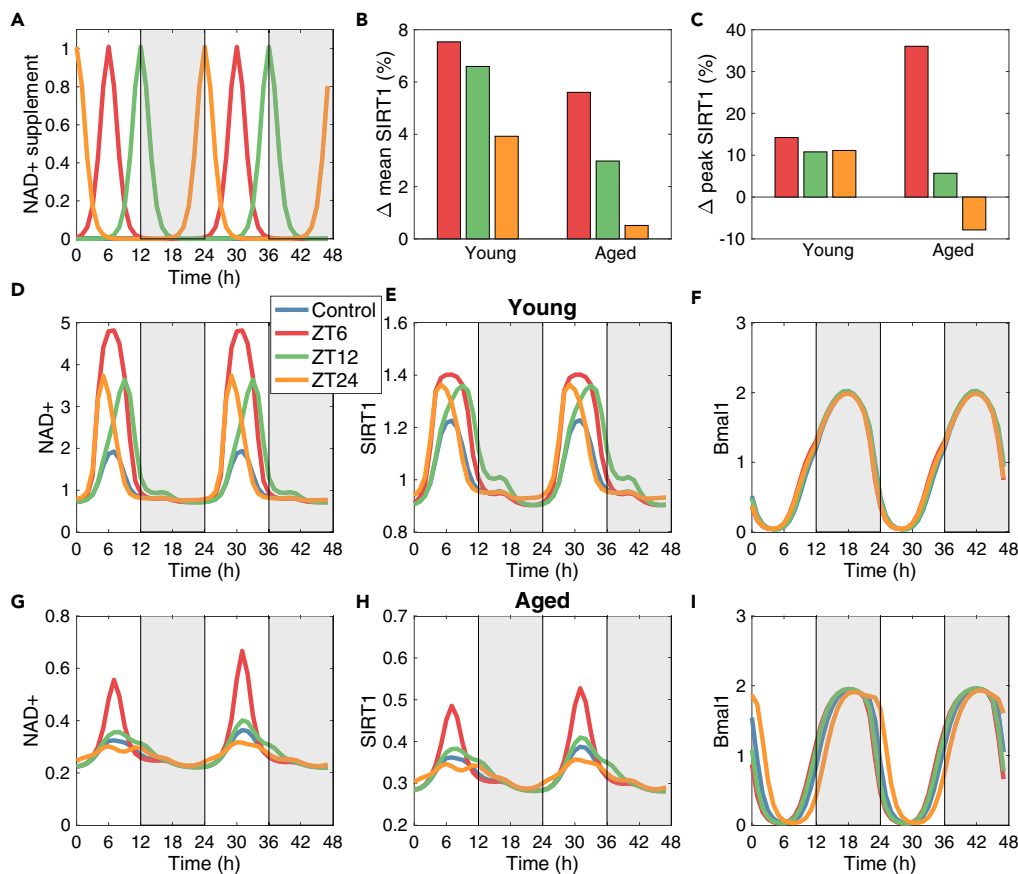
Figure 6. Effect of dosing schedule on NAD+ supplement efficacy

(A–I) Shown in arbitrary unit. Simulations are conducted for NAD+ supplement administered at ZT6, ZT12, and ZT24 (A), and in the young model (second row) and aged model (third row). NAD+ supplement has a major impact on the dynamics of NAD+ (D and G) and SIRT1 (E and H). Dosing schedule has a significant effect on drug efficacy in both the young and old models, as measured by mean SIRT1 (B) and peak SIRT1 (C).

(inactive) phase, almost immediately resets the phase of circadian gene expression in the liver (Stokkan et al., 2001; Damiola et al., 2000). Indeed, the liver circadian clock is one of the fastest tissue clocks to entrain to an altered feeding schedule, indicating that its coupling to food intake is stronger than to peripheral or central oscillators. To understand the mechanism that underlies this entrainment, we conduct a simulation of daytime and nighttime feeding. Simulation results indicate that the coupling of mTORC1 to the liver circadian clock, as formulated in the present model, is sufficient to explain its entrainment to an altered feeding schedule (Figure 3), although it should be acknowledgment that such entrainment may also be induced by a different connection not represented in the present model.

The interactions between metabolism and circadian rhythms in humans can be gleaned from clinical observations in shift workers. Shift work involves alternations in feeding schedule and other zeitgebers. A higher incidence of diabetes, obesity, and cardiovascular events has been reported among shift workers (Mukherji et al., 2019), although the underlying mechanisms have yet to be elucidated. Participants subjected to forced circadian misalignment (a simulation of shift work) have been found to exhibit insulin resistance and elevated blood pressure (Scheer et al., 2009). Our simulation of nighttime feeding (one aspect of shift work) predicts lowered phosphorylated Akt levels, compared to daytime feedback. Phosphorylated Akt is essential to the translocation of GLUT4; thus, our result suggests that nighttime feedback may lead to impaired glucose tolerance. It is noteworthy that patients with diabetes exhibit a dampened amplitude of circadian rhythms of insulin secretion (Boden et al., 1999) and glucose tolerance. Given this bidirectional nature of the relationship between circadian disruption and metabolic pathologies, circadian disruption may lead to a vicious cycle and contribute to the progression and worsening of metabolic diseases.

Aging and the circadian rhythms

Our model predicts a shortening of the liver circadian rhythm in aged mice (Figure 4). The effect of aging on the rhythmic expression of clock genes appears to be equivocal (Nakamura et al., 2015), with conflicting reports of shortening (Yamazaki et al., 2002) or lengthening of the SCN (Chang and Guarente, 2013), and an unaltered peripheral clock (Sato et al., 2017). An additional complication is that it is unclear to what extent these *in vitro* findings apply to a living organism. In particular, aging-related changes on the liver clock are likely masked by the feeding schedule. Nevertheless, in aging, a gradual decline is seen in a number of physiological functions, including the robustness of the circadian clock. Documented age-related changes in circadian rhythms include shortening of the circadian period (Morin, 1988; Pittendrigh and Daan, 1974; Weitzman et al., 1982; Witting et al., 1994), alteration in the phase angle of entrainment to the light/dark cycle (Morin, 1988; Scarbrough et al., 1997; Zee et al., 1992), fragmentation of the activity rhythm (Scarbrough et al., 1997), decreased precision in the onset of daily activity (Scarbrough et al., 1997; Zee et al., 1992), and alterations in the response to the phase-shifting effects of light(Rosenberg et al., 1991; Zhang et al., 1996) and nonphotic stimuli (Turek et al., 2007). These age-related changes in the circadian system may disrupt the proper phase relationships among numerous physiological and behavioral 24-hr rhythms, as well as between these rhythms and daily environmental cycles. The disruption of those relations may negatively impact the organism's health and its adaptation to the environment (Brock, 1991).

The interactions between aging and the circadian clock are complex and likely involve a bidirectional relationship (Kondratov et al., 2006; Krishnan et al., 2009; Nakahata et al., 2009). Possible mechanisms that contribute to the aging of the circadian clock include changes in the SCN, including its structure (Swaab et al., 1985; Zhou and Swaab, 1999), neuronal coupling (Satinoff et al., 1993; Masuda et al., 2018; Nakamura et al., 2011), and clock gene expression (Satinoff et al., 1993; Masuda et al., 2018; Nakamura et al., 2011). The present study focuses on the role of SIRT1 and NAD+. *In vitro*, SIRT1 regulates the acetylation of Bmal1 and Per*2* in the mouse liver (Nakahata et al., 2008; Asher et al., 2008) and human hepatocytes (Wang et al., 2016). SIRT1 expression in the mouse brain and liver decreases with age, and Sirt1 knockouts display a premature aging phenotype, including disrupted activity rhythms comparable to those in aged (19–22 months) wild-type mice (Chang and Guarente, 2013), as well as shortened lifespan and increased levels of proinflammatory markers in blood (Wang et al., 2016). The aged model in the present study predicts attenuated Bmal1, consistent with observations in a knockout of Sirt1 in the brain (Chang and Guarente, 2013), and a shortened circadian period (Figure 4). Taken together, model simulations and experimental findings concur on a role for an age-dependent decrease in SIRT1 activity in mediating changes in the molecular circadian clockwork (Yamazaki et al., 2002). Taken together, model simulations and experimental findings concur on a role for an age-dependent decrease in SIRT1 in mediating changes in the molecular circadian clockwork.

Circadian rhythm disturbances in the elderly are associated with a wide range of health conditions, including hypertension and cardiac insufficiency (Jensen et al., 1998), impaired immune functions and increased susceptibility to disease (Nikolich-Žugich, 2018), depression and poor cognitive and psychological functioning (Moe et al., 1995). Common treatments for circadian rhythm disorders in aging include the use of melatonin (Garzón et al., 2009) and light therapy (Mishima et al., 2018). Given the likely involvement of SIRT1 in the dysfunction of the circadian clock in aging, therapies that elevate SIRT1 activity may restore the circadian rhythms and reverse other age-related effects. In recent studies, supplementation of NAD+ intermediates such as nicotinamide mononucleotide (NMN) and NR was reported to dramatically reverse the effects of aging at the cellular and organismal levels (Gomes et al., 2013). Importantly, NAD+ intermediate supplementation appears to restore NAD+ levels in both nuclear and mitochondrial compartments of cells, and the benefits of NAD+ intermediate supplementation appear to be due to the reactivation of sirtuins. Given the role of the circadian clock in optimizing and maintaining health, some of the benefits of NAD+ intermediate supplementation may be attributed to the restoration of the circadian rhythms.

Dosing schedule and the circadian rhythms

In recent years, interest in resveratrol and NAD+ supplements has increased enormously after reports emerged on their benefits on metabolism and increased lifespan of various organisms (Howitz et al., 2003; Hashimoto et al., 2010). A key molecular target common to these drugs is SIRT1, which exhibits significant circadian variations (Wallace et al., 2018). Thus, a salient question is: *To what extent do dosing times*

impact the anti-aging effects of resveratrol and NAD+ supplements? Indeed, the circadian rhythms have been known to modulate drug pharmacokinetics and pharmacodynamics (Dallmann et al., 2014). Experimental data involving targeted anticancer agents have indicated that both circadian timing and drug dosage are critical factors in determining systemic exposure and thus pharmacological effects. For example, Everolimus, an immunosuppressant that inhibits mTOR, exerts a higher antitumor efficacy if taken at ZT12 compared to ZT0 (Okazaki et al., 2014). A link between dosing schedule and drug efficacy was also revealed for a number of other anticancer drugs (Li et al., 2012; Kloth et al., 2015; Zappe et al., 2015), analgesic (Johnson et al., 2014; Debruyne et al., 2014), antidiabetic drugs (Miyazaki et al., 2011), and antibiotics (Souayed et al., 2015).

The exact effect of dosing time on pharmacodynamics and pharmacokinetics depends on the drug and likely on patient characteristics. The present study focuses on one patient characteristic, age. We seek to answer the important clinical question: *Given the age of a patient, what is the best time to administer STACs or NAD+ supplements, to maximize the drugs' potential anti-aging effects?* The answer depends, first of all, on the measure of drug efficacy. If the goal is to elevate peak SIRT1 (to maximize physiological processes that activate above a SIRT1 threshold), then the best time to administer either STACs or NAD+ supplements is to coincide with the circadian peaks of NAD+ and SIRT1 in the control group (no drug), i.e., in the middle of the light periods (ZT6). If the goal is to maximize mean SIRT1, then the answer depends on the drug (STACs or NAD+ supplements) and on patient's age. For STACs, administering the drug in the young model at the beginning or end of the light periods (ZT12 or ZT24) yields a significant, albeit not drastic, improvement in terms of mean SIRT1, over administering it in the middle of the light periods (ZT6). The aged model is largely insensitive to dosing timing. For NAD+ supplements, administering the drug in the middle of the light periods (ZT6) yields the largest increase in mean SIRT1 in both models. These results are summarized in Figures 5 and 6, panels B and C.

A noteworthy finding of this study is that caution should be taken when STACs or NAD+ supplements are to be taken early in the morning (ZT24). For STACs, not only does this timing yield the smallest increase in peak SIRT1, it may also have an undesirable side effect of shifting the circadian clock (Figures 5F and 5I). The model predicts a 7-hr shift, although in practice other zeitgebers and inputs will likely render the circadian clock more robust. For NAD+ supplements, this timing generates the smallest increases in both mean and peak SIRT1, and in the aged population, it may even lower the SIRT1 peak.

Comparison with previous models and future extension

In a recent study (Guerrero-Morín and Santillán, 2020), Guerrero-Morín and Santillán studied the regulation of the circadian clock by coupling the minimal genetic oscillator model by Goodwin (Goodwin, 1965) with a simple mTORC1 activation model. That Goodwin model represents the feedback loop involving BMAL1, PER, and CRY, and can reproduce features of circadian oscillators such as light entrainment. However, it neglects the feedback loop involving BMAL1, REV-ERB, and ROR. That model (Guerrero-Morín and Santillán, 2020) only considers the unidirectional control of BMAL1 by mTROC1 but not the circadian regulation of metabolism, or the influence of other metabolic sensors (e.g., AMPK) on the circadian rhythms.

The goal of this study is to better understand the bidirectional interactions among metabolism and the circadian clock, and how those interactions changes in aging and pharmacological manipulation. To achieve that goal, we have developed a more comprehensive mathematical model of circadian rhythms and metabolism. We adopt the mammalian liver circadian clock model by Woller et al. (Woller et al., 2016). In addition to the dynamics of the core clock regulatory network, that model also incorporates metabolic sensors SIRT1 and AMPK, and represents additional mechanisms through which metabolism drives the clock. Specifically, the model (Woller et al., 2016) simulates the action of SIRT1 in modulating the transcriptional activity of CLOCK:BMAL1 and destabilizing PER2. SIRT1 also activates PGC1a, which coactivates ROR and increases Bmal1 expression. But before PGC1a can be deacetylated by SIRT1, phosphorylation by AMPK is required. Additionally, activated AMPK destabilizes PER and CRY.

Although the model by Woller et al. can predict how the activation of AMPK alters the circadian clock, (i) the AMPK level is assumed known *a priori*, and (ii) their model does not consider the role of mTORC1, which plays a central role in regulating fundamental cell processes, from protein synthesis to autophagy, and the signaling of which when dysregulated is implicated in the progression of cancer and diabetes, as

well as the aging process. Thus, we couple the circadian clock model (Woller et al., 2016) to our published model of insulin pathway (Sadria and Layton, 2021), which includes the insulin/IGF-1 pathway, mTORC1, and AMPK, and predicts how mTORC1, AMPK, and SIRT1 respond to variations in energy and nutrient abundance. The insulin pathway and mTORC1 model (Sadria and Layton, 2021) and the circadian clock model (Woller et al., 2016) are coupled by representing the increase of BMAL1 protein expression by mTORC1 (Lipton et al., 2017; Ramanathan et al., 2018), and the inhibition of mTORC1 phosphorylation by BMAL1 and PER2 (Wu et al., 2019).

The present model provides a state-of-the-art computational platform for investigating the interplay among aging, metabolism, and circadian rhythms. Model simulations have identified altered mTORC1 signaling as a mechanism leading to clock disruption and its associated metabolic effects, and suggested a pharmacological approach to resetting the clock in obesity and metabolic diseases. Further, mTORC1 signaling is switched on by a number of oncogenic signaling pathways and may be hyperactive in up to 70% of all human tumors (Forbes et al., 2010). Thus, there is much interest in targeting mTORC1 signaling as a potential therapeutic avenue for anticancer therapy. The potential effect of these treatments on the circadian clock may be studied using the present model.

Limitations of the study
A limitation of the present model is that it considers only the influence of variations in mTORC1, AMPK, and SIRT1, and neglects the influence of systemic signals from the SCN. This simplification is justified for the liver circadian clock, the entrainment phase of which is determined primarily by the feeding schedule. If the present model is to be adapted to other peripheral circadian clocks, the SCN inputs should be incorporated.

Resource availability
Lead contact
Information and requests for resources should be directed to and will be fulfilled by the lead contact, Mehrshad Sadria (msadria@uwaterloo.ca)

Materials availability
Not applicable.

Data and code availability
MATLAB programs used in the model simulations can be accessed at https://github.com/MehrshadSD/Clock-aging-and-metabolism.git.

METHODS
All methods can be found in the accompanying transparent methods supplemental file.

SUPPLEMENTAL INFORMATION
Supplemental information can be found online at https://doi.org/10.1016/j.isci.2021.102245.

AUTHOR CONTRIBUTIONS
Conceptualization, M.S. and A.T.L.; methodology, M.S. and A.T.L.; software, M.S. and A.T.L.; formal analysis, M.S. and A.T.L.; investigation, M.S. and A.T.L.; data curation, M.S. and A.T.L.; writing – original draft, M.S. and A.T.L.; writing – review & editing, M.S. and A.T.L.; visualization, M.S. and A.T.L.; funding acquisition, A.T.L.

DECLARATION OF INTERESTS
The authors declare no competing interests.

REFERENCES

Asher, G., Gatfield, D., Stratmann, M., Reinke, H., Dibner, C., Kreppel, F., Mostoslavsky, R., Alt, F.W., and Schibler, U. (2008). SIRT1 regulates circadian clock gene expression through PER2 deacetylation. Cell 134, 317–328.

Balsalobre, A., Damiola, F., and Schibler, U. (1998). A serum shock induces circadian gene expression in mammalian tissue culture cells. Cell 93, 929–937.

Boden, G., Chen, X., and Polansky, M. (1999). Disruption of circadian insulin secretion is associated with reduced glucose uptake in first-degree relatives of patients with type 2 diabetes. Diabetes 48, 2182–2188.

Bouchard, V.J., Rouleau, M., and Poirier, G.G. (2003). PARP-1, a determinant of cell survival in response to DNA damage. Exp. Hematol. 31, 446–454.

Braidy, N., Poljak, A., Grant, R., Jayasena, T., Mansour, H., Chan-Ling, T., Guillemin, G.J., Smythe, G., and Sachdev, P. (2014). Mapping NAD+ metabolism in the brain of ageing Wistar rats: potential targets for influencing brain senescence. Biogerontology 15, 177–198.

Brock, M.A. (1991). Chronobiology and aging. J. Am. Geriatr. Soc. 39, 74–91.

Chang, H.-C., and Guarente, L. (2013). SIRT1 mediates central circadian control in the SCN by a mechanism that decays with aging. Cell 153, 1448–1460.

Dallmann, R., Brown, S.A., and Gachon, F. (2014). Chronopharmacology: new insights and therapeutic implications. Annu. Rev. Pharmacol. Toxicol. 54, 339–361.

Damiola, F., Le Minh, N., Preitner, N., Kornmann, B., Fleury-Olela, F., and Schibler, U. (2000). Restricted feeding uncouples circadian oscillators in peripheral tissues from the central pacemaker in the suprachiasmatic nucleus. Genes Dev. 14, 2950–2961.

Debruyne, J.P., Weaver, D.R., and Dallmann, R. (2014). The hepatic circadian clock modulates xenobiotic metabolism in mice. J. Biol. Rhythms 29, 277–287.

Dibner, C., Schibler, U., and Albrecht, U. (2010). The mammalian circadian timing system: organization and coordination of central and peripheral clocks. Annu. Rev. Physiol. 72, 517–549.

Forbes, S.A., Bindal, N., Bamford, S., Cole, C., Kok, C.Y., Beare, D., Jia, M., Shepherd, R., Leung, K., and Menzies, A. (2010). COSMIC: mining complete cancer genomes in the Catalogue of Somatic Mutations in Cancer. Nucleic Acids Res. 39, D945–D950.

Garzón, C., Guerrero, J.M., Aramburu, O., and Guzmán, T. (2009). Effect of melatonin administration on sleep, behavioral disorders and hypnotic drug discontinuation in the elderly: a randomized, double-blind, placebo-controlled study. Aging Clin. Exp. Res. 21, 38–42.

Gomes, A.P., Price, N.L., Ling, A.J., Moslehi, J.J., Montgomery, M.K., Rajman, L., White, J.P., Teodoro, J.S., Wrann, C.D., and Hubbard, B.P. (2013). Declining NAD+ induces a pseudohypoxic state disrupting nuclear-mitochondrial communication during aging. Cell 155, 1624–1638.

Goodwin, B.C. (1965). Oscillatory behavior in enzymatic control processes. Adv. Enzyme Regul. 3, 425–437.

Guerrero-Morín, J.G., and Santillán, M. (2020). Crosstalk dynamics between the circadian clock and the mTORC1 pathway. J. Theor. Biol. 501, 110360.

Hashimoto, T., Horikawa, M., Nomura, T., and Sakamoto, K. (2010). Nicotinamide adenine dinucleotide extends the lifespan of Caenorhabditis elegans mediated by sir-2.1 and daf-16. Biogerontology 11, 31.

Howitz, K.T., Bitterman, K.J., Cohen, H.Y., Lamming, D.W., Lavu, S., Wood, J.G., Zipkin, R.E., Chung, P., Kisielewski, A., and Zhang, L.-L. (2003). Small molecule activators of sirtuins extend Saccharomyces cerevisiae lifespan. Nature 425, 191–196.

Hughes, M.E., Ditacchio, L., Hayes, K.R., Vollmers, C., Pulivarthy, S., Baggs, J.E., Panda, S., and Hogenesch, J.B. (2009). Harmonics of circadian gene transcription in mammals. PLoS Genet. 5, e1000442.

Imai, S.-I., and Guarente, L. (2014). NAD+ and sirtuins in aging and disease. Trends Cell Biol. 24, 464–471.

Jensen, E., Dehlin, O., Hagberg, B., Samuelsson, G., and Svensson, T. (1998). Insomnia in an 80-year-old population: relationship to medical, psychological and social factors. J. Sleep Res. 7, 183–189.

Johnson, B.P., Walisser, J.A., Liu, Y., Shen, A.L., Mcdearmon, E.L., Moran, S.M., Mcintosh, B.E., Vollrath, A.L., Schook, A.C., and Takahashi, J.S. (2014). Hepatocyte circadian clock controls acetaminophen bioactivation through NADPH-cytochrome P450 oxidoreductase. Proc. Natl. Acad. Sci. 111, 18757–18762.

Kaminsky, Y.G., Kosenko, E.A., and Kondrashova, M.N. (1984). Analysis of the circadian rhythm in energy metabolism of rat liver. Int. J. Biochem. 16, 629–639.

Khapre, R.V., Patel, S.A., Kondratova, A.A., Chaudhary, A., Velingkaar, N., Antoch, M.P., and Kondratov, R.V. (2014). Metabolic clock generates nutrient anticipation rhythms in mTOR signaling. Aging (Albany NY) 6, 675.

Kim, T.W., Jeong, J.-H., and Hong, S.-C. (2015). The impact of sleep and circadian disturbance on hormones and metabolism. Int. J. Endocrinol. 2015, 591729.

Kloth, J.S., Binkhorst, L., De Wit, A.S., De Bruijn, P., Hamberg, P., Lam, M.H., Burger, H., Chaves, I., Wiemer, E.A., and Van Der Horst, G.T. (2015). Relationship between sunitinib pharmacokinetics and administration time: preclinical and clinical evidence. Clin. Pharmacokinet. 54, 851–858.

Kondratov, R.V., Kondratova, A.A., Gorbacheva, V.Y., Vykhovanets, O.V., and Antoch, M.P. (2006). Early aging and age-related pathologies in mice deficient in BMAL1, the core componentof the circadian clock. Genes Dev. 20, 1868–1873.

Kondratova, A.A., and Kondratov, R.V. (2012). The circadian clock and pathology of the ageing brain. Nat. Rev. Neurosci. 13, 325–335.

Krishnan, N., Kretzschmar, D., Rakshit, K., Chow, E., and Giebultowicz, J.M. (2009). The circadian clock gene period extends healthspan in aging Drosophila melanogaster. Aging (Albany NY) 1, 937.

Li, Z., Yan, S., Attayan, N., Ramalingam, S., and Thiele, C.J. (2012). Combination of an allosteric Akt Inhibitor MK-2206 with etoposide or rapamycin enhances the antitumor growth effect in neuroblastoma. Clin. Cancer Res. 18, 3603–3615.

Lipton, J.O., Boyle, L.M., Yuan, E.D., Hochstrasser, K.J., Chifamba, F.F., Nathan, A., Tsai, P.T., Davis, F., and Sahin, M. (2017). Aberrant proteostasis of BMAL1 underlies circadian abnormalities in a paradigmatic mTOR-opathy. Cell Rep. 20, 868–880.

Massudi, H., Grant, R., Braidy, N., Guest, J., Farnsworth, B., and Guillemin, G.J. (2012a). Age-associated changes in oxidative stress and NAD+ metabolism in human tissue. PLoS One 7, e42357.

Massudi, H., Grant, R., Guillemin, G.J., and Braidy, N. (2012b). NAD+ metabolism and oxidative stress: the golden nucleotide on a crown of thorns. Redox Rep. 17, 28–46.

Masuda, T., Watanabe, Y., Fukuda, K., Watanabe, M., Onishi, A., Ohara, K., Imai, T., Koepsell, H., Muto, S., Vallon, V., and Nagata, D. (2018). Unmasking a sustained negative effect of SGLT2 inhibition on body fluid volume in the rat. Am. J. Physiol. Ren. Physiol. 315, F653–F664.

Millar-Craig, M., Bishop, C., and Raftery, E. (1978). Circadian variation of blood-pressure. The Lancet 311, 795–797.

Milne, J.C., Lambert, P.D., Schenk, S., Carney, D.P., Smith, J.J., Gagne, D.J., Jin, L., Boss, O., Perni, R.B., and Vu, C.B. (2007). Small molecule activators of SIRT1 as therapeutics for the treatment of type 2 diabetes. Nature 450, 712–716.

Mishima, E., Fukuda, S., Kanemitsu, Y., Saigusa, D., Mukawa, C., Asaji, K., Matsumoto, Y., Tsukamoto, H., Tachikawa, T., Tsukimi, T., et al. (2018). Canagliflozin reduces plasma uremic toxins and alters the intestinal microbiota composition in a chronic kidney disease mouse model. Am. J. Physiol. Ren. Physiol 315, F824–F833.

Miyazaki, M., Fujii, T., Takeda, N., Magotani, H., Iwanaga, K., and Kakemi, M. (2011). Chronopharmacological assessment identified GLUT4 as a responsible factor for the circadian variation of the hypoglycemic effect of tolbutamide in rats. Drug Metab. Pharmacokinet. 26, 503–515.

Moe, K.E., Vitiello, M.V., Larsen, L.H., and Prinz, P.N. (1995). Sleep/wake patterns in Alzheimer's disease: relationships with cognition and function. J. Sleep Res. 4, 15–20.

Morin, L.P. (1988). Age-related changes in hamster circadian period, entrainment, and rhythm splitting. J. Biol. Rhythms 3, 237–248.

Mukherji, A., Bailey, S.M., Staels, B., and Baumert, T.F. (2019). The circadian clock and liver function in health and disease. J. Hepatol. 71, 200–211.

Muller, J.E., Stone, P.H., Turi, Z.G., Rutherford, J.D., Czeisler, C.A., Parker, C., Poole, W.K., Passamani, E., Roberts, R., and Robertson, T. (1985). Circadian variation in the frequency of onset of acute myocardial infarction. New Engl. J. Med. 313, 1315–1322.

Nagoshi, E., Saini, C., Bauer, C., Laroche, T., Naef, F., and Schibler, U. (2004). Circadian gene expression in individual fibroblasts: cell-autonomous and self-sustained oscillators pass time to daughter cells. Cell 119, 693–705.

Nakahata, Y., Kaluzova, M., Grimaldi, B., Sahar, S., Hirayama, J., Chen, D., Guarente, L.P., and Sassone-Corsi, P. (2008). The NAD+-dependent deacetylase SIRT1 modulates CLOCK-mediated chromatin remodeling and circadian control. Cell 134, 329–340.

Nakahata, Y., Sahar, S., Astarita, G., Kaluzova, M., and Sassone-Corsi, P. (2009). Circadian control of the NAD+ salvage pathway by CLOCK-SIRT1. Science 324, 654–657.

Nakamura, T.J., Nakamura, W., Tokuda, I.T., Ishikawa, T., Kudo, T., Colwell, C.S., and Block, G.D. (2015). Age-related changes in the circadian system unmasked by constant conditions. eNeuro 2, ENEURO.0064-15.

Nakamura, T.J., Nakamura, W., Yamazaki, S., Kudo, T., Cutler, T., Colwell, C.S., and Block, G.D. (2011). Age-related decline in circadian output. J. Neurosci. 31, 10201–10205.

Nikolich-Žugich, J. (2018). The twilight of immunity: emerging concepts in aging of the immune system. Nat. Immunol. 19, 10–19.

Okazaki, H., Matsunaga, N., Fujioka, T., Okazaki, F., Akagawa, Y., Tsurudome, Y., Ono, M., Kuwano, M., Koyanagi, S., and Ohdo, S. (2014). Circadian regulation of mTOR by the ubiquitin pathway in renal cell carcinoma. Cancer Res. 74, 543–551.

Pittendrigh, C.S., and Daan, S. (1974). Circadian oscillations in rodents: a systematic increase of their frequency with age. Science 186, 548–550.

Ramanathan, C., Kathale, N.D., Liu, D., Lee, C., Freeman, D.A., Hogenesch, J.B., Cao, R., and Liu, A.C. (2018). mTOR signaling regulates central and peripheral circadian clock function. PLoS Genet. 14, e1007369.

Refinetti, R., and Menaker, M. (1992). The circadian rhythm of body temperature. Physiol. Behav. 51, 613–637.

Riera, C.E., Merkwirth, C., De Magalhaes Filho, C.D., and Dillin, A. (2016). Signaling networks determining life span. Annu. Rev. Biochem. 85, 35–64.

Robinson, J.L., Foustock, S., Chanez, M., Bois-Joyeux, B., and Peret, J. (1981). Circadian variation of liver metabolites and amino acids in rats adapted to a high protein, carbohydrate-free diet. J. Nutr. 111, 1711–1720.

Roenneberg, T., and Merrow, M. (1999). Circadian systems and metabolism. J. Biol. Rhythms 14, 449–459.

Rosenberg, R.S., Zee, P.C., and Turek, F.W. (1991). Phase response curves to light in young and old hamsters. Am. J. Physiol. 261, R491–R495.

Sadria, M., and Layton, A.T. (2021). Interactions among mTORC, AMPK, and SIRT: a computational model for cell energy balance and metabolism. Cell Comm. Signal.. https://www.biorxiv.org/content/10.1101/2020.10.07.330308v1.abstract

Satinoff, E., Li, H., Tcheng, T.K., Liu, C., Mcarthur, A., Medanic, M., and Gillette, M. (1993). Do the suprachiasmatic nuclei oscillate in old rats as they do in young ones? Am. J. Physiol. 265, R1216–R1222.

Sato, S., Solanas, G., Peixoto, F.O., Bee, L., Symeonidi, A., Schmidt, M.S., Brenner, C., Masri, S., Benitah, S.A., and Sassone-Corsi, P. (2017). Circadian reprogramming in the liver identifies metabolic pathways of aging. Cell 170, 664–677. e11.

Satoh, A., Imai, S.-I., and Guarente, L. (2017). The brain, sirtuins, and ageing. Nat. Rev. Neurosci. 18, 362.

Scarbrough, K., Losee-Olson, S., Wallen, E.P., and Turek, F.W. (1997). Aging and photoperiod affect entrainment and quantitative aspects of locomotor behavior in Syrian hamsters. Am. J. Physiol. 272, R1219–R1225.

Scheer, F.A., Hilton, M.F., Mantzoros, C.S., and Shea, S.A. (2009). Adverse metabolic and cardiovascular consequences of circadian misalignment. Proc. Natl. Acad. Sci. 106, 4453–4458.

Souayed, N., Chennoufi, M., Boughattas, F., Hassine, M., Attia, M.B., Aouam, K., Reinberg, A., and Boughattas, N.A. (2015). Circadian-time dependent tolerance and haematological toxicity to isoniazid in murine. Biomed. Pharmacother. 71, 233–239.

Stokkan, K.-A., Yamazaki, S., Tei, H., Sakaki, Y., and Menaker, M. (2001). Entrainment of the circadian clock in the liver by feeding. Science 291, 490–493.

Swaab, D.F., Fliers, E., and Partiman, T. (1985). The suprachiasmatic nucleus of the human brain in relation to sex, age and senile dementia. Brain Res. 342, 37–44.

Tulsian, R., Velingkaar, N., and Kondratov, R. (2018). Caloric restriction effects on liver mTOR signaling are time-of-day dependent. Aging (Albany NY) 10, 1640.

Turek, F.W., Penev, P., Zhang, Y., Van Reeth, O., Takahashi, J.S., and Zee, P. (2007). Alterations in the circadian system in advanced age. In Ciba Foundation Symposium 183-Circadian Clocks and Their Adjustment: Circadian Clocks and Their Adjustment: Ciba Foundation Symposium 183 (Wiley Online Library), pp. 212–234.

Wallace, E., Wright, S., Schoenike, B., Roopra, A., Rho, J.M., and Maganti, R.K. (2018). Altered circadian rhythms and oscillation of clock genes and sirtuin 1 in a model of sudden unexpected death in epilepsy. Epilepsia 59, 1527–1539.

Wang, R.-H., Zhao, T., Cui, K., Hu, G., Chen, Q., Chen, W., Wang, X.-W., Soto-Gutierrez, A., Zhao, K., and Deng, C.-X. (2016). Negative reciprocal regulation between Sirt1 and Per2 modulates the circadian clock and aging. Sci. Rep. 6, 1–15.

Weitzman, E.D., Moline, M.L., Czeisler, C.A., and Zimmerman, J.C. (1982). Chronobiology of aging: temperature, sleep-wake rhythms and entrainment. Neurobiol. Aging 3, 299–309.

Welsh, D.K., Takahashi, J.S., and Kay, S.A. (2010). Suprachiasmatic nucleus: cell autonomy and network properties. Annu. Rev. Physiol. 72, 551–577.

Witting, W., Mirmiran, M., Bos, N.P., and Swaab, D.F. (1994). The effect of old age on the free-running period of circadian rhythms in rat. Chronobiol. Int. 11, 103–112.

Woller, A., Duez, H., Staels, B., and Lefranc, M. (2016). A mathematical model of the liver circadian clock linking feeding and fasting cycles to clock function. Cell Rep. 17, 1087–1097.

Wu, R., Dang, F., Li, P., Wang, P., Xu, Q., Liu, Z., Li, Y., Wu, Y., Chen, Y., and Liu, Y. (2019). The circadian protein Period2 suppresses mTORC1 activity via recruiting Tsc1 to mTORC1 complex. Cell Metab. 29, 653–667. e6.

Yamazaki, S., Numano, R., Abe, M., Hida, A., Takahashi, R.-I., Ueda, M., Block, G.D., Sakaki, Y., Menaker, M., and Tei, H. (2000). Resetting central and peripheral circadian oscillators in transgenic rats. Science 288, 682–685.

Yamazaki, S., Straume, M., Tei, H., Sakaki, Y., Menaker, M., and Block, G.D. (2002). Effects of aging on central and peripheral mammalian clocks. Proc. Natl. Acad. Sci. 99, 10801–10806.

Yoo, S.-H., Yamazaki, S., Lowrey, P.L., Shimomura, K., Ko, C.H., Buhr, E.D., Siepka, S.M., Hong, H.-K., Oh, W.J., and Yoo, O.J. (2004). PERIOD2::LUCIFERASE real-time reporting of circadian dynamics reveals persistent circadian oscillations in mouse peripheral tissues. Proc. Natl. Acad. Sci. 101, 5339–5346.

Yoshino, J., Baur, J.A., and Imai, S.-I. (2018). NAD+ intermediates: the biology and therapeutic potential of NMN and NR. Cell Metab. 27, 513–528.

Zappe, D.H., Crikelair, N., Kandra, A., and Palatini, P. (2015). Time of administration important? Morning versus evening dosing of valsartan. J. Hypertens. *33*, 385.

Zee, P.C., Rosenberg, R.S., and Turek, F.W. (1992). Effects of aging on entrainment and rate of resynchronization of circadian locomotor activity. Am. J. Physiol. *263*, R1099–R1103.

Zhang, Y., Kornhauser, J., Zee, P.C., Mayo, K.E., Takahashi, J., and Turek, F.W. (1996). Effects of aging on light-induced phase-shifting of circadian behavioral rhythms, fos expression and CREB phosphorylation in the hamster suprachiasmatic nucleus. Neuroscience *70*, 951–961.

Zhou, J.N., and Swaab, D.F. (1999). Activation and degeneration during aging: a morphometric study of the human hypothalamus. Microsc. Res. Tech. *44*, 36–48.

Supplemental information

Aging affects circadian clock and metabolism

and modulates timing of medication

Mehrshad Sadria and Anita T. Layton

Transparent Methods

The present model is a combination of two published models. Main model components include the insulin/IGF-1 and mTOR signaling pathway (Sadria and Layton, 2021), the core circadian clock pathway (Woller et al., 2016), and key metabolism regulators AMPK, NAD+, and SIRT1. The dynamics of the signaling pathways are modelled as a system of ODEs. Figure 1 depicts the pathways and protein interactions. The reactions and associated parameters are presented in Tables S1 and S2. Terms have been added to describe the coupling between the metabolism and clock components; those terms are highlighted in the equations. New parameters that characterize the coupling between the energy/metabolic pathways and the circadian system are shown in Table S3. While the original models have been individually validated (Woller et al., 2016, Sadria and Layton, 2021), selected parameters of the new coupled model must be adjusted to ensure a satisfactory fit with experimental data (Woller et al., 2016, Khapre et al., 2014). The agreement between predicted clock protein and mTORC1 profiles with experimental data is illustrated in Fig. 2. The adjusted parameters are shown in Table S4. Parameter fitting was performed using the interior point optimization method in MATLAB. Values for the other parameters can be found in Refs. (Woller et al., 2016, Sadria and Layton, 2021, Dalle Pezze et al., 2014).

Within the insulin/IGF-1 signaling and mTOR pathways, insulin activates the insulin receptor (IR), which triggers the IRS and PI3K, resulting in the phosphorylation of PDK1 and mTORC2, respectively. mTORC2 phosphorylates AKT on the S473 and T308 residues, whereas PDK1 activates AKT. Active AKT phosphorylates a variety of proteins, including TSC1_TSC2 and PRAS40. Phosphorylation of TSC1_TSC2 by AKT inactivates the TSC complex, thereby activating mTORC1 and resulting in a number of downstream effects, including the repression of the autophagy pathway and elevation of core clock protein BMAL1. A detailed description of the insulin/IGF-1 signaling and mTOR pathway model can be found in Refs. (Dalle Pezze et al., 2014, Sadria and Layton, 2021).

The clock model comprises several transcription factors that regulate gene expression: period (Per), cryptochromes (Cry), Rev-Erg and ROR-related orphan receptor retinoic acid receptor-related orphan receptor (Ror), brain and muscle ARNT-Like 1 (Bmal1), and circadian locomotor output cycles kaput (CLOCK). These core clock components exhibit circadian oscillations, driven by a network of interlocked transcriptional-translational feedback loops. In the primary negative feedback loop, CLOCK and BMAL1 heterodimerize to initiate the transcription of target clock genes, including Per (with isoforms Per1, Per2, Per3) and Cry (with isoforms Cry1 and

Cry2), by binding the E-box elements in the promoter region (Dibner et al., 2010, Zheng et al., 2001). PERs and CRYs then heterodimerize to inhibit their own transcription by acting on CLOCK:BMAL1 protein complex. In the secondary feedback loop, activators of CLOCK and BMAL1 dimerize to initiate the transcription of Rev-Erbα and Ror(Preitner et al., 2002, Triqueneaux et al., 2004). REV-ERBs and RORs are shown to repress and activate Bmal1 transcription, respectively (Liu et al., 2008, Cho et al., 2012, Guillaumond et al., 2005). In addition, Rev-Erb also inhibits Cry transcription to ensure robust oscillations (Relógio et al., 2011, Bugge et al., 2012). Following the approach in Ref. (Woller et al., 2016), we represent the two period homologs (Per1 and Per2) as a single Per gene and ignore Per3, and we represent the two cryptochromes (Cry1, Cry2) as a single Cry gene.

Circadian rhythms play a critical role in the physiological processes involved in energy metabolism and energy balance. In turn, mTORC1 regulates the proteostasis of the core clock protein BMAL1, affecting its translation, degradation, and subcellular localization(Lipton et al., 2017). Thus, activation of mTORC1 results in elevated levels of BMAL1, and vice versa (Lipton et al., 2017, Ramanathan et al., 2018). In a negative feedback loop, BMAL1 inhibits the phosphorylation of mTORC1, as does another core clock protein PER2 (Wu et al., 2019). SIRT1 triggers the deacetylation of PGC1-α, the deacetylation of CLOCK-BMAL1 complex, and the degradation of PER2. AMPK accelerates the phosphorylation of PGC1-α, as well as the degradation of PER2 and CRY1. Deacetylated and phosphorylated PGC1-α increases the generation rate of Bmal1 genes. These reactions are described by the coupling terms highlighted in Table S1.

Table S1. **Model equations: Metabolic signaling pathway. Related to Figure 1.**

The bidirectional influence between the metabolism and circadian pathways is represented by (new) coupling terms that are highlighted in the ODE associated with mTORC1_pS2448, mTORC1, Prot_bmal, and CB.

$$\frac{d[\text{IR}\beta]}{dt} = \begin{aligned}&+(par\_IR\_beta\_ready * [\text{IR}\beta\_\text{refractory}]) \\ &-([\text{IR}\beta] * par\_IR\_beta\_phos\_by\_Insulin * [\text{Insulin}])\end{aligned}$$

$$\frac{d[\text{IR}\beta\_\text{pY1146}]}{dt} = \begin{aligned}&+([\text{IR}\beta] * par\_IR\_beta\_phos\_by\_Insulin * [\text{Insulin}]) \\ &-(par\_IR\_beta\_pY1146\_dephos * [\text{IR}\beta\_\text{pY1146}])\end{aligned}$$

$$\frac{d[\text{IR}\beta\_\text{refractory}]}{dt} = \begin{aligned}&+(par\_IR\_beta\_pY1146\_dephos * [\text{IR}\beta\_\text{pY1146}]) \\ &-(par\_IR\_beta\_ready * [\text{IR}\beta\_\text{refractory}])\end{aligned}$$

$$\frac{d[\text{mTORC1\_pS2448}]}{dt} = \begin{aligned}&-([\text{TSC1\_TSC2}] + [\text{TSC1\_TSC2\_pS1387}]) * [\text{mTORC1\_pS2448}] * par\_mTORC1\_pS2448\_dephos\_by\_TSC1\_TSC2) \\ &-(b\_pras\_mtorc1 * [\text{mTORC1\_pS2448}] * 10^{\wedge}(0.25 * [\text{PRAS40}])) \\ &-([\text{mTORC1\_pS2448}] * [\text{Act\_ULK1}] * 0.00016) \\ &+ [\text{Amino\_Acid}] * [\text{mTORC1}] * par\_mTORC1\_S2448\_activation\_by\_Amino\_Acids \\ &* \left(\frac{mTORC1_{Vmax} * ([leucine\_a] + [leucine\_conc])}{[leucine\_a] + [leucine\_conc] + [sestrin2]}\right) \\ &-\boxed{(par\_bmal\_mTORC1 * [Prot\_bmal] + par\_per\_mTORC1 * [Prot\_per])[mTORC1]}\end{aligned}$$

$$\frac{d[\text{mTORC1}]}{dt} = \begin{aligned}&+([\text{TSC1\_TSC2}] + [\text{TSC1\_TSC2\_pS1387}]) * [\text{mTORC1\_pS2448}] * par\_mTORC1\_pS2448\_dephos\_by\_TSC1\_TSC2) \\ &+(b\_pras\_mtorc1 * [\text{mTORC1\_pS2448}] * 10^{\wedge}(0.25 * [\text{PRAS40}])) \\ &+([\text{mTORC1\_pS2448}] * [\text{Act\_ULK1}] * 0.00016) \\ &- [\text{Amino\_Acid}] * [\text{mTORC1}] * par\_mTORC1\_S2448\_activation\_by\_Amino\_Acids \\ &* \left(\frac{mTORC1_{Vmax} * ([leucine\_a] + [leucine\_conc])}{[leucine\_a] + [leucine\_conc] + [sestrin2]}\right) \\ &+\boxed{(par\_bmal\_mTORC1 * [Prot\_bmal] + par\_per\_mTORC1 * [Prot\_per])[mTORC1]}\end{aligned}$$

$$\frac{d[\text{mTORC2}]}{dt} = \begin{aligned}&-([\text{Amino\_Acid}] * [\text{mTORC2}] * par\_mTORC2\_S2481\_phos\_by\_Amino\_Acids) \\ &-([\text{PI3K\_p}] * [\text{mTORC2}] * par\_mTORC2\_S2481\_phos\_by\_PI3K\_variant\_p) \\ &+(par\_mTORC2\_pS2481\_dephos * [\text{mTORC2\_pS2481}])\end{aligned}$$

$$\frac{d[\text{mTORC2\_pS2481}]}{dt} = \begin{aligned}&+([\text{Amino\_Acid}] * [\text{mTORC2}] * par\_mTORC2\_S2481\_phos\_by\_Amino\_Acids) \\ &+([\text{PI3K\_p}] * [\text{mTORC2}] * par\_mTORC2\_S2481\_phos\_by\_PI3K\_variant\_p) \\ &-(par\_mTORC2\_pS2481\_dephos * [\text{mTORC2\_pS2481}])\end{aligned}$$

$$\frac{d[\text{IRS}]}{dt} = \begin{aligned}&-([\text{Amino\_acid}] * [\text{IRS}] * par\_IRS\_phos\_by\_Amino\_Acids) \\ &-([\text{IRS}] * par\_IRS\_phos\_by\_IR\_beta\_pY1146 * [\text{IR}\beta\_\text{pY1146}]) \\ &-([\text{IRS}] * par\_IRS\_phos\_by\_p70\_S6K\_pT229\_pT389 * \\ &[\text{p70\_S6K\_pT229\_pT389}]) \\ &+(par\_IRS\_pS636\_turnover * [\text{IRS\_pS636}])\end{aligned}$$

$$\frac{d[\text{IRS\_p}]}{dt} = \begin{aligned}&+([\text{Amino\_Acid}] * [\text{IRS}] * par\_IRS\_phos\_by\_Amino\_Acids) \\ &+([\text{IRS}] * par\_IRS\_phos\_by\_IR\_beta\_pY1146 * [\text{IR}\beta\_\text{pY1146}]) \\ &-([\text{IRS\_p}] * par\_IRS\_p\_phos\_by\_p70\_S6K\_pT229\_pT389 * [\text{p70S6K\_pT229\_pT389}])\end{aligned}$$

$$\frac{d[\text{IRS\_pS636}]}{dt} = \begin{aligned}&+([\text{IRS\_p}] * par\_IRS\_p\_phos\_by\_p70\_S6K\_pT229\_pT389 * [\text{p70S6K\_pT229\_pT389}]) \\ &+([\text{IRS}] * par\_IRS\_phos\_by\_p70\_S6K\_pT229\_pT389 * [\text{p70S6K\_pT229\_pT389}]) \\ &-(par\_IRS\_pS636\_turnover * [\text{IR\_pS636}])\end{aligned}$$

$$\frac{d[\text{TSC1\_TSC2}]}{dt} = \begin{aligned}&-([\text{AMPK\_pT172}] * [\text{TSC1\_TSC2}] * par\_TSC1\_TSC2\_S1387\_phos\_by\_AMPK\_pT172) \\ &-(([\text{AKT\_pT308}] + [\text{AKT\_pT3089\_pS473}]) * [\text{TSC1\_TSC2}] * par\_TSC1\_TSC2\_T1462\_phos\_by\_Akt\_pT308) \\ &+(par\_TSC1\_TSC2\_pS1387\_dephos * [\text{TSC1\_TSC2\_pS1387}]) \\ &+(par\_TSC1\_TSC2\_pT1462\_dephos * [\text{TSC1\_TSC2\_pT1462}])\end{aligned}$$

$$\frac{d[\text{TSC1\_TSC2\_pT1462}]}{dt} = \begin{aligned}&+(([\text{Akt-pT308}] +[\text{Akt\_pT308\_pS473}])^*[\text{TSC1\_TSC2}] * par\_TSC1\_TSC2\_T1462\_phos\_by\_Akt\_pT308)\\&-(par\_TSC1\_TSC2\_pT1462\_dephos * [\text{TSC1\_TSC2\_pT1462}])\end{aligned}$$

$$\frac{d[\text{TSC1\_TSC2\_pS1387}]}{dt} = \begin{aligned}&+([\text{AMPK-pT172}]^* [\text{TSC1\_TSC2}] * par\_TSC1\_TSC2\_S1387\_phos\_by\_AMPK\_pT172)\\&-(par\_TSC1\_TSC2\_pS1387\_dephos * [\text{TSC1\_TSC2\_pS1387}])\end{aligned}$$

$$\frac{d[\text{PRAS40}]}{dt} = \begin{aligned}&-([\text{PRAS40}] * par\_PRAS40\_S183\_phos\_by\_mTORC1\_pS2448\_first * [\text{mTORC1\_pS2448}])\\&-(([\text{Akt\_pT308}]+ [\text{Akt\_pT308\_pS473}]) * [\text{PRAS40}] * par\_PRAS40\_T246\_phos\_by\_Akt\_pT308\_first)\\&+(par\_PRAS40\_pS183\_dephos\_first * [\text{PRAS40\_pS183}])\\&+(par\_PRAS40\_pT246\_dephos\_first * [\text{PRAS40\_pT246}])\end{aligned}$$

$$\frac{d[\text{PRAS40\_pS183}]}{dt} = \begin{aligned}&+([\text{PRAS40}] * par\_PRAS40\_S183\_phos\_by\_mTORC1\_pS2448\_first * [\text{mTORC1\_pS2448}])\\&-(([\text{Akt\_pT308}]+ [\text{Akt\_pT308\_pS473}])^*[\text{PRAS40\_pS183}] * par\_PRAS40\_T246\_phos\_by\_Akt\_pT308\_second)\\&-(par\_PRAS40\_pS183\_dephos\_first * [\text{PRAS40\_pS183}])\\&+(par\_PRAS40\_pT246\_dephos\_second * [\text{PRAS40\_pT246\_pS183}])\end{aligned}$$

$$\frac{d[\text{PRAS40\_pT246}]}{dt} = \begin{aligned}&-(par\_PRAS40\_S183\_phos\_by\_mTORC1\_pS2448\_second * [\text{PRAS40\_pT246}]^* [\text{mTORC1\_pS2448}])\\&-(par\_PRAS40\_pT246\_dephos\_first * [\text{PRAS40\_pT246}])\\&+([\text{Akt\_pT308}]^* [\text{Akt\_pT308\_pS473}]^* [\text{PRAS40}] * par\_PRAS40\_T246\_phos\_by\_Akt\_pT308\_first)\\&+(par\_PRAS40\_pS183\_dephos\_second * [\text{PRAS40\_pT246\_pS183}])\end{aligned}$$

$$\frac{d[\text{PRAS40\_pT246\_pS183}]}{dt} = \begin{aligned}&+(([\text{Akt\_pT308}]+ [\text{Akt\_pT308\_pS473}])^*[\text{PRAS40\_pS183}] * par\_PRAS40\_T246\_phos\_by\_Akt\_pT308\_second)\\&+(par\_PRAS40\_S183\_phos\_by\_mTORC1\_pS2448\_second * [\text{PRAS40\_pT246}]^* [\text{mTORC1\_pS2448}])\\&-(par\_PRAS40\_pS183\_dephos\_second * [\text{PRAS40\_pT246\_pS183}])\\&-(par\_PRAS40\_pT246\_dephos\_second * [\text{PRAS40\_pT246\_pS183}])\end{aligned}$$

$$\frac{d[\text{AKT}]}{dt} = \begin{aligned}&-([\text{AKT}] * par\_Akt\_T308\_phos\_by\_PI3K\_p\_PDK1\_first * [\text{PDK1\_p}])\\&-([\text{AKT}] * par\_Akt\_S473\_phos\_by\_mTORC2\_pS2481\_first * [\text{mTORC2\_pS2481}])\\&+(par\_Akt\_pT308\_dephos\_first * [\text{Akt\_pT308}])\\&+(par\_Akt\_pS473\_dephos\_first * [\text{Akt\_pS473}])\end{aligned}$$

$$\frac{d[\text{Akt\_pT308\_pS473}]}{dt} = \begin{aligned}&+(par\_Akt\_T308\_phos\_by\_PI3K\_p\_PDK1\_second * [\text{Akt\_pS473}]^* [\text{PDK1\_p}])\\&+(par\_Akt\_S473\_phos\_by\_mTORC2\_pS2481\_second * [\text{Akt\_pT308}]^*[\text{mTORC2\_pS2481}])\\&-(par\_Akt\_pT308\_dephos\_first * [\text{Akt\_pT308}])\\&-(par\_Akt\_pS473\_dephos\_second * [\text{Akt\_pT308\_pS473}])\end{aligned}$$

$$\frac{d[\text{Akt\_pT308}]}{dt} = \begin{aligned}&+([AKT] * par\_Akt\_T308\_phos\_by\_PI3K\_p\_PDK1\_first * [PDK1\_p])\\&-(par\_Akt\_S473\_phos\_by\_mTORC2\_pS2481\_second * [Akt\_pT308] * [mTORC2\_pS2481])\\&-(par\_Akt\_pT308\_dephos\_first * [Akt\_pT308])\\&+(par\_Akt\_pS473\_dephos\_second * [Akt\_pT308\_pS473])\end{aligned}$$

$$\frac{d[\text{Akt\_pS473}]}{dt} = \begin{aligned}&+(par\_Akt\_pS473\_dephos\_second * [AKT\_pT308\_pS473])\\&-(par\_Akt\_pT308\_dephos\_first * [AKT\_pT308])\\&+(par\_PI3K\_PDK1\_phos\_by\_IRS\_p * [AKT] * [PI3K\_p\_PDK1])\\&-(par\_Akt\_S473\_phos\_by\_mTORC2\_pS2481\_first) * [AKT\_pT308] * [mTORC2\_pS2481])\end{aligned}$$

$$\frac{d[\text{p70S6K}]}{dt} = \begin{aligned}&-([\text{PDK1\_p}]^* [\text{p70S6K}] * par\_p70\_S6K\_T229\_phos\_by\_PI3K\_p\_PDK1\_first)\\&-([\text{mTORC1\_pS2448}]^* [\text{p70S6K}] * par\_p70\_S6K\_T389\_phos\_by\_mTORC1\_pS2448\_first)\\&+(par\_p70\_S6K\_pT229\_dephos\_first * [\text{p70S6K\_pT229}])\\&+(par\_p70\_S6K\_pT389\_dephos\_first * [\text{p70S6K\_pT389}])\end{aligned}$$

$$\frac{d[\text{p70S6K\_pT229}]}{dt} = \begin{aligned}&+([\text{PDK1\_p}]^*[\text{p70S6K}] * par\_p70\_S6K\_T229\_phos\_by\_PI3K\_p\_PDK1\_first)\\&-([\text{mTORC1\_pS2448}] * par\_p70\_S6K\_T389\_phos\_by\_mTORC1\_pS2448\_second * [\text{p70S6K\_pT229}])\\&+(par\_p70\_S6K\_pT389\_dephos\_second * [\text{p70S6K\_pT229\_pT389}])\\&-(par\_p70\_S6K\_pT229\_dephos\_first * [\text{p70S6K\_pT229}])\end{aligned}$$

$$\frac{d[\text{p70S6K\_pT389}]}{dt} = \begin{aligned}&+([\text{mTORC1\_pS2448}]^* [\text{p70S6K}] * par\_p70\_S6K\_T389\_phos\_by\_mTORC1\_pS2448\_first)\\&-([\text{PDK1\_p}] * par\_p70\_S6K\_T229\_phos\_by\_PI3K\_p\_PDK1\_second * [\text{p70S6K\_pT389}])\\&-(par\_p70\_S6K\_pT389\_dephos\_first * [\text{p70S6K\_pT389}])\end{aligned}$$

$$+(par\_p70\_S6K\_pT229\_dephos\_second * [p70S6K\_pT229\_pT389])$$

$$\frac{d[\textbf{p70S6K\_pT389\_pT229}]}{dt} = \begin{aligned}&+([PDK1\_p] * par\_p70\_S6K\_T229\_phos\_by\_PI3K\_p\_PDK1\_second * [p70S6K\_pT389])\\&+([mTORC1\_pS2448] * par\_p70\_S6K\_T389\_phos\_by\_mTORC1\_pS2448\_second * [p70S6K\_pT229])\\&-(par\_p70\_S6K\_pT229\_dephos\_second * [p70S6K\_pT229\_pT389])\\&-(par\_p70\_S6K\_pT389\_dephos\_second * [p70S6K\_pT229\_pT389])\end{aligned}$$

$$\frac{d[\textbf{PI3K}]}{dt} = \begin{aligned}&+(par\_PI3K\_variant\_p\_dephos * [PI3K\_p])\\&-([IR\beta\_pY1146]*[PI3K] * par\_PI3K\_variant\_phos\_by\_IR\_beta\_pY1146)\end{aligned}$$

$$\frac{d[\textbf{PI3K\_p}]}{dt} = \begin{aligned}&-(par\_PI3K\_variant\_p\_dephos * [PI3K\_p])\\&+([IR\beta\_pY1146]*[PI3K] * par\_PI3K\_variant\_phos\_by\_IR\_beta\_pY1146)\end{aligned}$$

$$\frac{d[\textbf{PDK1}]}{dt} = \begin{aligned}&+(par\_PI3K\_p\_PDK1\_dephos * [PDK1\_p])\\&-([IRS\_p]* [PDK1] * par\_PI3K\_PDK1\_phos\_by\_IRS\_p)\end{aligned}$$

$$\frac{d[\textbf{PDK1\_p}]}{dt} = \begin{aligned}&-(par\_PI3K\_p\_PDK1\_dephos * [PDK1\_p])\\&+([IRS\_p]* [PDK1] * par\_PI3K\_PDK1\_phos\_by\_IRS\_p)\end{aligned}$$

$$\frac{d[\textbf{AMPK}]}{dt} = \begin{aligned}&-(100 * [AMPK] * par\_AMPK\_T172\_phos\_by\_AminoAcids * [leucine\_conc] * [sestrine\_conc])\\&-([AMPK] * par\_AMPK\_T172\_phos * [IRS\_p])\\&+(par\_AMPK\_pT172\_dephos * [AMPK\_pT172])\\&-(ksirt * [Act\_SIRT]*[AMPK])\\&+([Act\_ULK1]*[AMPK\_pT172] * kUKAP)\end{aligned}$$

$$\frac{d[\textbf{AMPK\_pT172}]}{dt} = \begin{aligned}&+(100 * [AMPK] * par\_AMPK\_T172\_phos\_by\_AminoAcids * [leucine\_conc] * [sestrine\_conc])\\&+([AMPK] * par\_AMPK\_T172\_phos * [IRS\_p])\\&-(par\_AMPK\_pT172\_dephos * [AMPK\_pT172])\\&+(ksirt * [Act\_SIRT] * [AMPK])\\&-([Act\_ULK1] * [AMPK\_pT172] * kUKAP)\end{aligned}$$

$$\frac{d[\textbf{ULK1}]}{dt} = -k10 * [ULK1] * [AMPK\_pT172] + kULKd * [Act\_ULK1] + KULKM * [Act\_ULK1] * [mTORC1\_pS2448]$$

$$\frac{d[\textbf{AC\_ULK1}]}{dt} = +k10 * [ULK1] * [AMPK\_pT172] - kULKd * [Act\_ULK1] - KULKM * [Act\_ULK1] * [mTORC1\_pS2448]$$

Table S2. **Model equations: Circadian clock. Related to Figure 1.**

The bidirectional influence between the metabolism and circadian pathways is represented by (new) coupling terms that are highlighted in the ODE associated with mTORC1_pS2448, mTORC1, Prot_bmal, and CB.

$$\frac{d[\text{per}]}{dt} = \begin{aligned}&-dm\_per * [per] \\ &+ \left(\frac{Vmax\_per * \left(1 + fold\_per * \left(\frac{[CB]}{Ka\_per\_cb * (1 + Act\_SIRT)}\right)^{hill\_per\_cb}\right)}{1 + \left(\frac{[CB]}{Ka\_per\_cb * (1 + Act\_SIRT)}\right)^{hill\_per\_cb} * \left(1 + \left(\frac{[PC]}{Ki\_per\_pc}\right)^{hill\_per\_pc}\right)}\right)\end{aligned}$$

$$\frac{d[\text{cry}]}{dt} = \begin{aligned}&-dm\_cry * [cry] \\ &+ \left(\frac{Vmax\_cry * \left(1 + fold\_cry * \left(\frac{[CB]}{Ka\_cry\_cb * (1 + \text{Act\_SIRT})}\right)^{hill\_cry\_cb}\right)}{1 + \left(\frac{[CB]}{Ka\_cry\_cb * (1 + \text{Act\_SIRT})}\right)^{hill\_cry\_cb} * \left(1 + \left(\frac{[PC]}{Ki\_cry\_pc}\right)^{hill\_cry\_pc}\right)} * \frac{1}{1 + \left(\frac{[\text{Prot\_rev}]}{Ki\_cry\_rev}\right)^{hill\_cry\_rev}}\right)\end{aligned}$$

$$\frac{d[\text{rev}]}{dt} = \begin{aligned}&-dm\_rev * [rev] \\ &+ \left(\frac{Vmax\_rev * \left(1 + fold\_rev * \left(\frac{[CB]}{Ka\_rev\_cb * (1 + \text{Act\_SIRT})}\right)^{hill\_rev\_cb}\right)}{1 + \left(\frac{[CB]}{Ka\_rev\_cb * (1 + \text{Act\_SIRT})}\right)^{hill\_rev\_cb} * \left(1 + \left(\frac{[PC]}{Ki\_rev\_pc}\right)^{hill\_rev\_pc}\right)}\right)\end{aligned}$$

$$\frac{d[\text{ror}]}{dt} = \begin{aligned}&-dm\_ror * [ror] \\ &+ \left(\frac{Vmax\_ror * \left(1 + fold\_ror * \left(\frac{[CB]}{Ka\_ror\_cb * (1 + \text{Act\_SIRT})}\right)^{hill\_ror\_pc}\right)}{1 + \left(\frac{[CB]}{Ka\_ror\_pc * (1 + \text{Act\_SIRT})}\right)^{hill\_ror\_cb} * \left(1 + \left(\frac{[PC]}{Ki\_ror\_pc}\right)^{hill\_ror\_pc}\right)}\right)\end{aligned}$$

$$\frac{d[\text{bmal}]}{dt} = \begin{aligned}&-dm\_bmal * [bmal] \\ &+ \left(\frac{Vmax\_bmal * \left(1 + fold\_bmal * (1 + \text{Act\_PGC1a}) * \left(\frac{[\text{Prot\_ror}]}{Ka\_bmal\_ror}\right)^{hill\_bmal\_ror}\right)}{1 + \left(\frac{[\text{Prot\_rev}]}{Ki\_bmal\_rev}\right)^{hill\_bmal\_rev} + \left(\frac{[\text{Prot\_ror}]}{Ka\_bmal\_ror}\right)^{hill\_bmal\_ror}}\right)\end{aligned}$$

$$\frac{d[\text{Prot\_per}]}{dt} = \begin{aligned}&-dp\_per * (1 + m\_per\_sirt * \text{Act\_SIRT} + m\_per\_ampk * \text{Act\_AMPK}) \\ &\qquad\qquad * [\text{Prot\_per}] \\ &+ kp\_per * [per] \\ &-(kass\_pc * [\text{Prot\_cry}] * [\text{Prot\_per}] - kdiss\_pc * [PC])\end{aligned}$$

$$\frac{d[\text{Prot\_cry}]}{dt} = \begin{aligned}&-dp\_cry * (1 + m\_cry\_ampk * \text{Act\_AMPK}) * [\text{Prot\_cry}] \\ &+ kp\_per * [cry] \\ &-(kass\_pc * [\text{Prot\_cry}] * [\text{Prot\_per}] - kdiss\_pc * [PC])\end{aligned}$$

$$\frac{d[\text{Prot\_rev}]}{dt} = \begin{aligned}&-dp\_rev * [\text{Prot\_rev}] \\ &+ kp\_rev * [rev]\end{aligned}$$

$$\frac{d[\text{Prot\_ror}]}{dt} = \begin{aligned}&-dp\_ror * [\text{Prot\_ror}] \\ &+ kp\_ror * [ror]\end{aligned}$$

$$\frac{d[\textbf{Prot\_bmal}]}{dt} = \begin{array}{l} -\textbf{\textit{dp\_bmal}}[\text{Prot\_bmal}] \\ + \textbf{\textit{kp\_bmal}} * [\text{bmal}] \\ -(\textbf{\textit{kass\_cb}} * [\text{Prot\_bmal}] - \textbf{\textit{kdiss}}_{\textbf{\textit{cb}}} * [\text{CB}]) \\ \colorbox{yellow}{$+(\textbf{\textit{par\_mTORC1\_bmal}} * [\textbf{\textit{Prot\_bmal}}] * [\textbf{\textit{mTORC1}}])$} \end{array}$$

$$\frac{d[\textbf{PC}]}{dt} = \begin{array}{l} +(\textbf{\textit{kass\_pc}} * [\text{Prot\_cry}] * [\text{Prot\_per}] - \textbf{\textit{kdiss\_pc}} * [\text{PC}]) \\ -\textbf{\textit{dp\_pc}} * [\text{PC}] \end{array}$$

$$\frac{d[\textbf{CB}]}{dt} = \begin{array}{l} +(\textbf{\textit{kass\_cb}} * [\text{Prot\_bmal}] - \textbf{\textit{kdiss\_cb}} * [\text{CB}]) \\ -\textbf{\textit{dp\_cb}} * [\text{CB}] \\ \colorbox{yellow}{$-(\textbf{\textit{par\_mTORC1\_cb}} * [\textbf{\textit{CB}}] * [\textbf{\textit{mTORC1}}])$} \end{array}$$

$$\frac{d[\textbf{nampt}]}{dt} = \begin{array}{l} -\textbf{\textit{dm\_nampt}} * [\text{nampt}] \\ + \left(\dfrac{\textbf{\textit{Vmax\_nampt}} * \left(1 + \textbf{\textit{fold\_nampt}} * \left(\dfrac{[\text{CB}]}{\textbf{\textit{Ka\_nampt\_cb}} * (1 + \text{Act\_SIRT})}\right)^{\textbf{\textit{hill\_nampt\_cb}}}\right)}{1 + \left(\dfrac{[\text{CB}]}{\textbf{\textit{Ka\_nampt\_cb}} * (1 + \text{Act\_SIRT})}\right)^{\textbf{\textit{hill\_nampt\_cb}}} * \left(1 + \left(\dfrac{[\text{PC}]}{\textbf{\textit{Ki\_nampt\_pc}}}\right)^{\textbf{\textit{hill\_nampt\_pc}}}\right)} \right) \end{array}$$

$$\frac{d[\textbf{Prot\_nampt}]}{dt} = \begin{array}{l} -\dfrac{\textbf{\textit{dp\_nampt}} * [\text{Prot\_nampt}]}{1 + \textbf{\textit{m\_nampt\_ampk}} * \text{Act\_AMPK}} \\ +\textbf{\textit{kp\_nampt}} * [\text{nampt}] \end{array}$$

$$\frac{d[\textbf{NAD}]}{dt} = \begin{array}{l} -\left(\dfrac{\textbf{\textit{d\_nad}} * ([\text{NAD}] - \textbf{\textit{NAD\_basal}})}{\textbf{\textit{Knad}} + [\text{NAD}] - \textbf{\textit{NAD\_basal}}}\right) \\ +\left(\dfrac{\textbf{\textit{Vmax\_nad}} * [\text{Prot\_nampt}] * ([\text{NAD}] - \textbf{\textit{NAD\_basal}})}{\textbf{\textit{Knam}} + \textbf{\textit{NAD\_tot}} - [\text{NAD}]}\right) \end{array}$$

$$\frac{d[\textbf{dbp}]}{dt} = \begin{array}{l} -\textbf{\textit{dm\_dbp}} * [\textbf{\textit{dbp}}] \\ + \left(\dfrac{\textbf{\textit{Vmax\_dbp}} * \left(1 + \textbf{\textit{fold\_dbp}} * \left(\dfrac{[\text{CB}]}{\textbf{\textit{Ka\_dbp\_cb}} * (1 + \text{Act\_SIRT})}\right)^{\textbf{\textit{hill\_dbp\_cb}}}\right)}{1 + \left(\dfrac{[\text{CB}]}{\textbf{\textit{Ka\_dbp\_cb}} * (1 + \text{Act\_SIRT})}\right)^{\textbf{\textit{hill\_dbp\_cb}}} * \left(1 + \left(\dfrac{[\text{PC}]}{\textbf{\textit{Ki\_dbp\_pc}}}\right)^{\textbf{\textit{hill\_dbp\_pc}}}\right)} \right) \end{array}$$

$$\textbf{Act\_SIRT} = \dfrac{\textbf{\textit{Csirt}} * \textbf{\textit{Vsirt}} * [\text{NAD}]}{\textbf{\textit{Ksirt}} + [\text{NAD}]}$$

$$\textbf{Act\_PGC1a} = \dfrac{\textbf{\textit{Cpgc1}} * \textbf{\textit{Vpg}} * \text{Act\_AMPK} * \text{Act\_SIRT} * \text{Prot\_TGC1a}}{1 + \dfrac{\text{Act\_AMPK}}{\textbf{\textit{Kpg1}}} * \left(1 + \dfrac{\text{Act\_SIRT}}{\textbf{\textit{Kpg2}}}\right)}$$

Table S3. Model parameters coupling the insulin/IGF-1 and mTOR signaling pathway and the core circadian clock pathway. Related to Figure 1.

| Symbol	Description	Value
par_bmal_mTORC1	Inhibitory effect of BMAL1 on mTORC1	0.0118
par_per_mTORC1	Inhibitory effect of PER2 on mTORC1	0.0104
par_mTORC1_bmal	Activating effect of mTORC1 on BMAL1	0.0104
par_mTORC1_cb	Inhibitory effect of mTORC1 on CLOCK-BMAL1	0.0261

Table S4. Selected model parameters that have been modified from published studies(Dalle Pezze et al., 2014, Woller et al., 2016, Sadria and Layton, 2021). Related to Figure 1.

Symbol	Description	Value
par_bmal_mTORC1	Inhibitory effect of BMAL1 on mTORC1	0.0118
par_per_mTORC1	Inhibitory effect of PER2 on mTORC1	0.0104
par_mTORC1_bmal	Activating effect of mTORC1 on BMAL1	0.0104
par_mTORC1_cb	Inhibitory effect of mTORC1 on CLOCK-BMAL1	0.0261
kp_bmal	Translation rate constant from Bmal1 mRNA to BMAL1 protein	0.5405
dp_bmal	Degradation rate of BMAL1 protein	0.2252
$kass\_cb$	Association rate constant of CLOCK-BMAL! complex	0.0151
$kdiss\_cb$	Disassociation rate constant of CLOCK-BMAL! complex	0.0066
d_cb	Degradation rate of CLOCK-BMAL1	0.0849
kp_per	Translation rate constant from Per2 mRNA to PER2 protein	3.9968
dp_per	Degradation rate of PER2 protein	56.1535
dm_per	Degradation rate of Per2 mRNA	0.3005
$Vmax\_per$	Generation rate constant of Per1 mRNA	0.8032
kp_cry	Translation rate constant from Cry1 mRNA to CRY1 protein	14.0871
dp_cry	Degradation rate of CRY1 protein	0.6536
$kass\_pc$	Association rate constant of PER-CRY complex	13.2884
$kdiss\_pc$	disassociation rate constant of PER-CRY complex	0.0261
kp_rev	Translation rate constant from Rev-Erb mRNA to REV-ERB protein	0.0641
kp_ror	Translation rate constant from Ror mRNA to ROR protein	0.3677
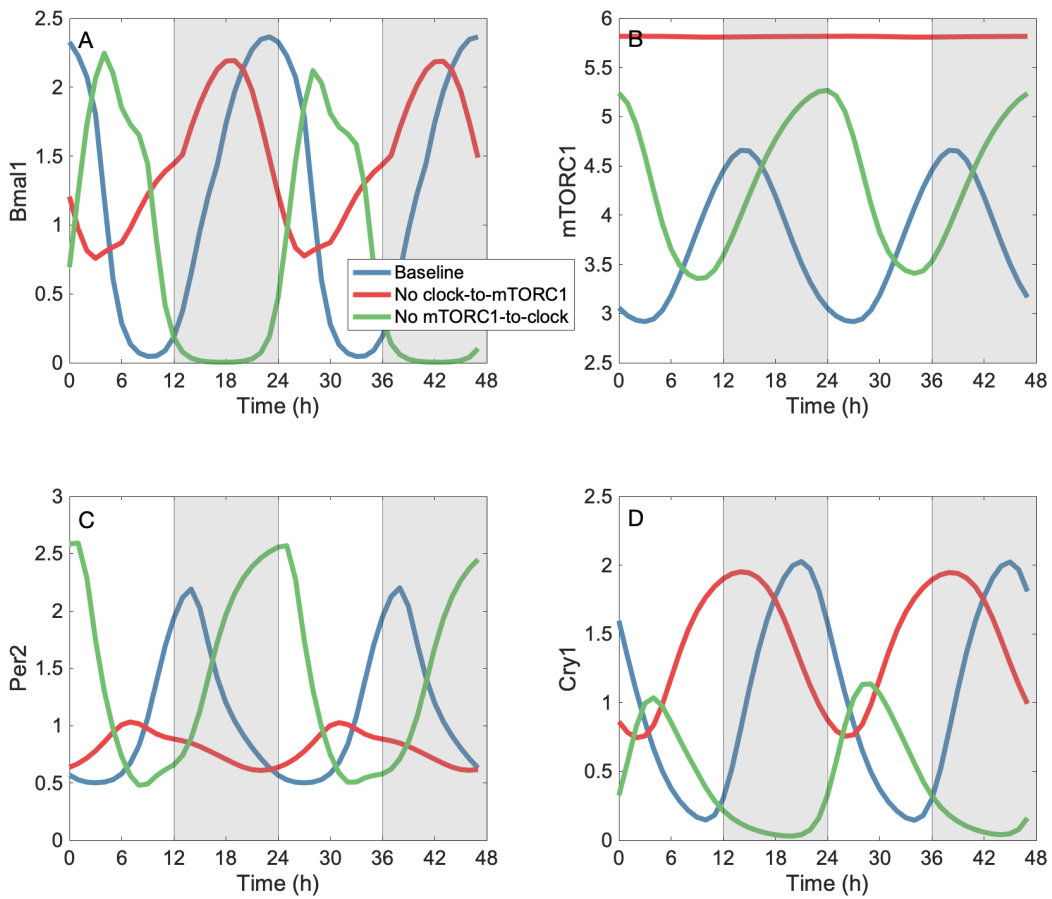
Figure S1. Effect of mTORC1 and core clock gene coupling. Related to Figure 2.
Predicted oscillations in Bmal1 mRNA, mTORC1, Per2, and Cry1, obtained with intact coupling (baseline, blue curves), without inhibitory effects of BMAL1 and PER2 on mTORC1 (red curves), and without activating effect of mTORC1 on BMAL1 and CLOCK-BMAL1 (green curves).
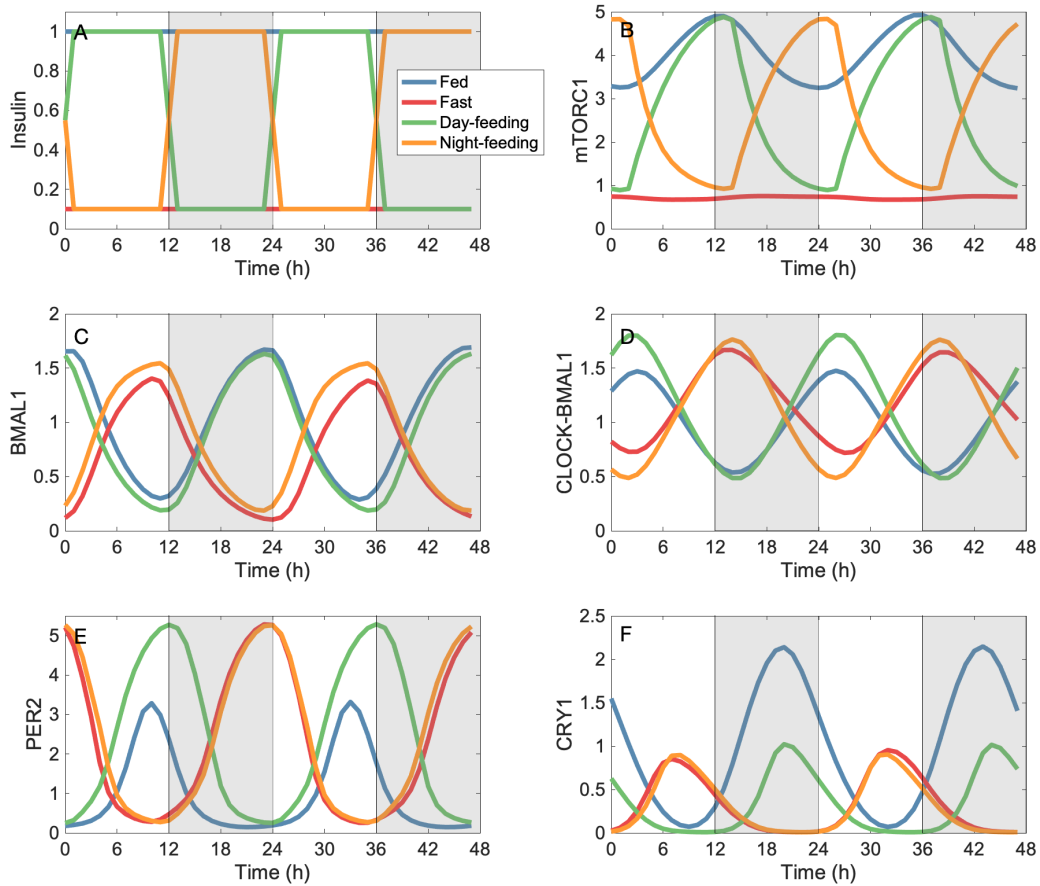
Figure S2. Effects of feeding schedule on mTORC1 and core clock gene levels, obtained for the aged model. Related to Figure 3.
A, insulin levels for a fed-like state (constant at 1), a fasted-like state (constant at 0.1), day-time feeding, and night-time feeding. *B*, mTORC1 levels, driven to oscillate by the clock and feeding schedule, and elevated at high insulin levels. *C-F*, core clock protein time-profiles.

BUGGE, A., FENG, D., EVERETT, L. J., BRIGGS, E. R., MULLICAN, S. E., WANG, F., JAGER, J. & LAZAR, M. A. 2012. Rev-erbα and Rev-erbβ coordinately protect the circadian clock and normal metabolic function. *Genes & development,* 26**,** 657-667.

CHO, H., ZHAO, X., HATORI, M., RUTH, T. Y., BARISH, G. D., LAM, M. T., CHONG, L.-W., DITACCHIO, L., ATKINS, A. R. & GLASS, C. K. 2012. Regulation of circadian behaviour and metabolism by REV-ERB-α and REV-ERB-β. *Nature,* 485**,** 123-127.

DALLE PEZZE, P., NELSON, G., OTTEN, E. G., KOROLCHUK, V. I., KIRKWOOD, T. B., VON ZGLINICKI, T. & SHANLEY, D. P. 2014. Dynamic modelling of pathways to cellular senescence reveals strategies for targeted interventions. *PLoS Comput Biol,* 10**,** e1003728.

DIBNER, C., SCHIBLER, U. & ALBRECHT, U. 2010. The mammalian circadian timing system: organization and coordination of central and peripheral clocks. *Annual review of physiology,* 72**,** 517-549.

GUILLAUMOND, F., DARDENTE, H., GIGUÈRE, V. & CERMAKIAN, N. 2005. Differential control of Bmal1 circadian transcription by REV-ERB and ROR nuclear receptors. *Journal of biological rhythms,* 20**,** 391-403.

KHAPRE, R. V., PATEL, S. A., KONDRATOVA, A. A., CHAUDHARY, A., VELINGKAAR, N., ANTOCH, M. P. & KONDRATOV, R. V. 2014. Metabolic clock generates nutrient anticipation rhythms in mTOR signaling. *Aging (Albany NY),* 6**,** 675.

LIPTON, J. O., BOYLE, L. M., YUAN, E. D., HOCHSTRASSER, K. J., CHIFAMBA, F. F., NATHAN, A., TSAI, P. T., DAVIS, F. & SAHIN, M. 2017. Aberrant proteostasis of BMAL1 underlies circadian abnormalities in a paradigmatic mTOR-opathy. *Cell reports,* 20**,** 868-880.

LIU, A. C., TRAN, H. G., ZHANG, E. E., PRIEST, A. A., WELSH, D. K. & KAY, S. A. 2008. Redundant function of REV-ERBα and β and non-essential role for Bmal1 cycling in transcriptional regulation of intracellular circadian rhythms. *PLoS Genet,* 4**,** e1000023.

PREITNER, N., DAMIOLA, F., ZAKANY, J., DUBOULE, D., ALBRECHT, U. & SCHIBLER, U. 2002. The orphan nuclear receptor REV-ERBα controls circadian transcription within the positive limb of the mammalian circadian oscillator. *Cell,* 110**,** 251-260.

RAMANATHAN, C., KATHALE, N. D., LIU, D., LEE, C., FREEMAN, D. A., HOGENESCH, J. B., CAO, R. & LIU, A. C. 2018. mTOR signaling regulates central and peripheral circadian clock function. *PLoS genetics,* 14**,** e1007369.

RELÓGIO, A., WESTERMARK, P. O., WALLACH, T., SCHELLENBERG, K., KRAMER, A. & HERZEL, H. 2011. Tuning the mammalian circadian clock: robust synergy of two loops. *PLoS Comput Biol,* 7**,** e1002309.

SADRIA, M. & LAYTON, A. T. 2021. Interactions among mTORC, AMPK, and SIRT: A Computational Model for Cell Energy Balance and Metabolism. *Cell Comm Signal*.

TRIQUENEAUX, G., THENOT, S., KAKIZAWA, T., ANTOCH, M. P., SAFI, R., TAKAHASHI, J. S., DELAUNAY, F. & LAUDET, V. 2004. The orphan receptor Rev-erbα gene is a target of the circadian clock pacemaker. *Journal of molecular endocrinology,* 33**,** 585-608.

WOLLER, A., DUEZ, H., STAELS, B. & LEFRANC, M. 2016. A mathematical model of the liver circadian clock linking feeding and fasting cycles to clock function. *Cell reports,* 17**,** 1087-1097.

WU, R., DANG, F., LI, P., WANG, P., XU, Q., LIU, Z., LI, Y., WU, Y., CHEN, Y. & LIU, Y. 2019. The circadian protein Period2 suppresses mTORC1 activity via recruiting Tsc1 to mTORC1 complex. *Cell metabolism,* 29**,** 653-667. e6.

ZHENG, B., ALBRECHT, U., KAASIK, K., SAGE, M., LU, W., VAISHNAV, S., LI, Q., SUN, Z. S., EICHELE, G. & BRADLEY, A. 2001. Nonredundant roles of the mPer1 and mPer2 genes in the mammalian circadian clock. *Cell,* 105**,** 683-694.